Appendix.

Relation between the Velocity of Propagation and the Amplitude of Seismic Waves.

It is well known fact that, in any earthquake, the principal shocks are preceded by tremors of small amplitudes. On the supposition that the waves of the tremors and of the principal shocks are all generated simultaneously at one and the same orgin, the above facts shows that the velocities of tremors are much greater than that of the principal shocks. Indeed, according to Professor Ōmori,* the velocities of the first and second tremors are equal to 12.8 and 7.2 kilometres per second, while that of the principal shocks is only 3.3 kilometres per second.

The cause of such a wide difference between the velocities in seismic waves must probably be of much complicated nature. In so far, however, as the velocity of propagation of elastic wave is determined by the ratio of the elastic constants to density, it is a matter of course that the existence of the elastic yielding can never be put out of consideration in the determination of the velocity. Moreover, the strain is far beyond the limit of elasticity, I think, even in the weakest earthquake. If this is the case, the effect of elastic yielding would be, at least, one of the principal causes of the diminution of velocity.

There will exist, it is true, neither pure longitudinal nor pure transversal waves in the actual case. Moreover, the modulus of rigidity would have but little to do with the seismic waves. It would thus be too bold to say anything about the velocity of seismic waves from the observations on the modulus of rigidity alone. But possibly other elastic constants also will be of similar nature. These premised,

* F. Ōmori. The velocities of transit of the seismic waves deduced from the observations of recent large Japanese earthquakes in Italy and Germany. Publications of the E. Investigation Committee in Foreign Languages. No. 5. pp. 71–80. 1901.

I give the following explanation for the wide difference between the velocities of seismic waves.

To begin with, in Table II, β represents obviously the increase of twist per unit increase of couple in arbitrary unit; i. e. the modulus of rigidity is inversely proportional to β. Whence it follows that, as the velocity is proportional to the square root of the modulus of rigidity, it is also inversely proportional to the square root of β. Then, the ratios of the velocities in several conditions will be as follows.

TABLE IX. (*Velocity of propagation.*)

Rock	Serpentine		Pyroxenite	
Amplitude	$\sqrt{\beta}$	$\frac{v}{v_0}$	$\sqrt{\beta}$	$\frac{v}{v_0}$
* {0.025} 0.0* Kilogram	0.565	1.00	0.499	1.00
0.4	0.651	0.78	0.428	0.73
1.0	0.696	0.73	0.497	0.71
1.5	0.713	0.71	0.504	0.70
2.4	0.716	0.71	0.529	0.69
3.0	0.726	0.70		

From the above table, it is obvious that, even in the case where Hooke's law holds, as the figures in Pls. IV and V. show, the velocity of propagation rapidly decreases when the amount of distortion increases.

Further effect may be seen from the following theoretical investigation. The velocity diminishes when the amplitude increases, but it increases when the medium is in the strained state.

Diminution of Velocity in virtue of the Increase of Amplitude:— In page 45, it was shown that $\triangle_p\ {}_{\lambda\cdot\cdot A+1}\eta_p$ is greater than $\triangle_p\ {}_{\lambda\cdot\cdot A}\eta_p$, which proves the said statement. Here it will be sufficient to give one numerical example. In the equation (11) given in page 44 put $p=0$ and $\lambda=1$, then

$$\triangle_{p\ 1.A}\gamma_0 = k \log \frac{\{8A+1\}[5A+1]^2[A+1]^2}{[7A+1][3A+1]^2} = k \log 10.\ L \qquad \text{say.}$$

This value of $\triangle_{p\ 1.A}\gamma_0$, expressed as a function of the amplitude A, represents the amount of the increase of twist, due to elastic yielding, per unit increase of couple in the stage of zero-couple after one cycle of twisting to and fro through amplitude A. Its actual value for several amplitudes are given in the following table.

TABLE X. (*Velocity of propagation*).

A	1	2	3	4	5	6	7	8	9	10
L	0.1022	0.2247	0.3255	0.4083	0.4784	0.5383	0.5919	0.6393	0.6821	0.7211
$\frac{v}{v_0}$; $\left\{\frac{k}{\tau_0}=1.38\right\}$	1.00	0.96	0.94	0.92	0.91	0.90	0.89	0.88	0.87	0.86
$\frac{v}{v_0}$; $\left\{\frac{k}{\tau_0}=6.91\right\}$	1.00	0.83	0.81	0.77	0.73	0.70	0.68	0.67	0.65	0.64
$\frac{v}{v_0}$; $\left\{k \text{ very great}\right\}$.	1.00	0.68	0.55	0.50	0.46	0.44	0.42	0.40	0.39	0.38

As it was discussed in former section, if τ_0 is the amount of twist obeying Hooke's law, the actual amount of twist is

$$\tau = \tau_0 + \triangle_{p\ \lambda.A}\gamma_p.$$

Then, v and c being the velocity and factor of proportionality respectively, we have

$$v = c\{\tau_0 + \triangle_{p\cdot\ \lambda.A}\gamma_p\}^{-\frac{1}{2}} = v_0\{1 + \frac{k}{\tau_0}\log f(A)\}^{-\frac{1}{2}}.$$

When the elastic yielding is very small, it may be neglected so that

$$v = v_0$$

i. e. v_0 is the velocity of wave through a stratum of rocks which is perfectly elastic or has no elastic yielding. In this case alone, velocity remains unchanged for all waves of different amplitudes; Otherwise, $\frac{v}{v_0}$ diminishes when the amplitude increases. For marble, specimen No. 6_2, a piece of metamorphised sedimentary rock of Pàlæozoic age, as it was found from the experiments whose result is shown in Fig 31, Pl. XV., approximate value of $\frac{k}{\tau_0}$ is 1.38. Adopting this value of $\frac{k}{\tau_0}$, for the ratio of velocities, I obtained those given in the third row of the above table. Those in the last row correspond to the case where the part obeying Hooke's law is negligibly small compared with that due to the elastic yielding. For the intermediate one, I add those in the fourth row.

Increase of Velocity in virtue of the rock's having been initially strained:— In page 48 the relation was proved

$$\triangle_{p\,j+1}\eta_{j+1} < \triangle_{p\cdot j}\eta_j\,,$$

which proves the said statement. The following numerical example will show clearly. In the equation (19) put $N=1$, $\mathfrak{n}=1$, $\lambda=1$ and $\mathfrak{N}=10$ so that $\alpha=49$, then we have

$$\triangle_{p\cdot j}\eta_j = k\log\frac{\{49-j\}[19-j]^2[6]^2[2]^2}{[39-j]^2[8]^2[4]^2} = k\log 10.\ L \qquad \text{say.}$$

Here $\triangle_{pj}\eta_j$, expressed as a function of j, represents the amount of the decrease of twist, due to elastic recovery, per unit withdrawal of the applied couple in the stage specified by j, (it having been initially subjected to couple given by $\mathfrak{N}$) after one cycle round that stage. For different values of j, the corresponding values of $\triangle_{pj}\eta_j$ are given in the following table, together with the ratio of velocities in the marble above stated.

TABLE XI. *(Velocity of Propagation).*

j	0	1	2	3	4	5	6	7	8	9
L	0.2136	0.1802	0.1445	0.1064	0.0652	0.0207	−0.0277	−0.0606	−0.1392	−0.2041
$\frac{n}{n_c}$; $\left\{\frac{k}{\tau_0}=1.38\right\}$	1.00	1.01	1.02	1.03	1 04	1.05	1.07	1.08	1.10	1.13

Here also, the velocity remains constant only within the rocks in which no elastic yielding and consequently no elastic recovery exists.

Numerical values of the velocity of transversal wave propagating through several rocks, as calculated by the formula

$$\text{velocity} = \sqrt{\left\{ \frac{\text{Modulus of rigidity}}{\text{Dencity}} \right\}},$$

are given in the last column of Table VIII. Different values for one and the same specimen correspond to the different conditions,—*i. e.* whether the rock is in the neutral or is in the twisted state—and different amplitudes of the wave to be propagated.

Summary.

From what has been above discussed, it may be safely said that, of several waves, one whose amplitude is smaller has necessarily greater velocity than the ther, in so far as the medium through which the elastic wave propagates is liable to elastic yielding. When the yielding predominates, the velocity may become two or three times smaller as the amplitude becomes some ten times greater. Also when the medium is in the strained state, e. g. along mountain-chain, the velocity is much greater than in ordinary case. The latter variation, however, is much smaller than the former.

Lastly, it must be remarked that the elastic yielding is never an only cause which gives rise to torsional hysteresis. Complete expression for hysteresis must contain, at least, one more term which is independent of time. For illustration of this last statement, magnetic hysteresis gives best example, in which magnetic yielding is negligibly small. In magnetic hysteresis, indeed, the predominating term is wholly independent of time. Such term as above, also, would possibly exist in torsional hysteresis. If this term could be known and taken into account, then it would lead to a satisfactory explanation for the wide difference between the velocities of the tremors and of the principal shocks. If this is not wholly out of conception, then it would be more natural than to assume two different paths for the two kinds of seismic waves. At the epicentre, the tremors may last only for a short time, but the duration will be lengthened proportionally as the distance increases. The disturbance of smallest amplitude will first make its appearance as the beginning of the preliminary tremor, followed by waves of greater amplitudes in succession. Other disturbances propagating through different strata would probably make their appearance intermixed with the former, giving somewhat irregular record on the seismograph. Complete description of the nature of elastic hysteresis requires further investigation.

In conclusion, I wish to express my great indebtedness to Mr. Fukuchi for valuable information concerning the geological and petrological character of rocks examined in the present experiment. My best thanks are due to Professor H. Nagaoka and also to Professor A. Tanakadate, without whose valuable advice and most kind guidance I could scarecely have succeeded in carrying out this experiment.

TABLE XII. {*Time-lag*}.

$\frac{\tau}{\tau_0^1}$	$\frac{t}{k \log 10}$
0.00001	0.0020
0.0001	0.0063
0.001	0.0207
0.01	0.0656
0.03	0.1150
0.05	0.1493
0.07	0.1775
0.1	0.2139
0.2	0.3113
0.3	0.3936
0.4	0.4710
0.5	0.5487
0.55	0.5889
0.60	0.6308
0.65	0.6752
0.70	0.7231
0.75	0.7759
0.80	0.8361
0.85	0.9077
0.90	1.000
0.95	1.140
0.96	1.182
0.97	1.234
0.98	1.303
0.99	1.414
0.995	1.517
0.9995	1.817
0.99995	2.074
etc.	etc.
1.00	∞

TABLE XIII. {*Elastic Recovery*}.

t'	$\frac{\rho}{k \log 10}$
0	0.000
1	0.760
2	1.175
3	1.665
4	1.974
5	2.229
6	2.444
7	2.629
8	2.789
9	2.930
10	3.055
11	3.167
12	3.268
13	3.359
14	3.451
15	3.517
17	3.650
19	3.765
22	3.907
25	4.025
30	4.182
35	4.305
40	4.400
45	4.479
50	4.545
60	4.638
70	4.725
80	4.785
etc.	etc.
∞	5.267

TABLE XIV. {*Elastic yielding*}.

p	$\log_{10}\Gamma\{p+1\}$	p	$\log_{10}\Gamma\{p+1\}$	p	$\log_{10}\Gamma\{p+1\}$	p	$\log_{10}\Gamma\{p+1\}$
1	0.0000	26	26.6056	51	66.1906	76	111.2754
2	0.3010	27	28.0370	52	67.9066	77	113.1619
3	0.7782	28	29.4841	53	69.6309	78	115.0539
4	1.3802	29	30.9465	54	71.3633	79	116.9516
5	2.0792	30	32.4236	55	73.1036	80	118.8547
6	2.8573	31	33.9150	56	74.8518	81	120.7632
7	3.7024	32	35.4202	57	76.6077	82	122.6770
8	4.6055	33	36.9387	58	78.3711	83	124.5960
9	5.5598	34	38.4701	59	80.1420	84	126.5203
10	6.5598	35	40.0142	60	81.9201	85	128.4497
11	7.6012	36	41.5705	61	83.7055	86	130.3842
12	8.6803	37	43.1387	62	85.4979	87	132.3238
13	9.7943	38	44.7185	63	87.2972	88	134.2682
14	10.9404	39	46.3096	64	89.1034	89	136.2176
15	12.1165	40	47.9116	65	90.9163	90	138.1719
16	13.3206	41	49.5244	66	92.7358	91	140.1309
17	14.5511	42	51.1476	67	94.5619	92	142.0947
18	15.8063	43	52.7811	68	96.3944	93	144.0632
19	17.0851	44	54.4246	69	98.2333	94	146.0363
20	18.3861	45	56.0778	70	100.0784	95	148.0140
21	19.7083	46	57.7405	71	101.9296	96	149.9963
22	21.0508	47	59.4126	72	103.7869	97	151.9831
23	22.4125	48	61.0939	73	105.6503	98	153.9743
24	23.7927	49	62.7841	74	107.5195	99	155.9699
25	25.1906	50	64.4830	75	109.3946	100	157.9699

TABLE XV. (1). {*Hysteresis Function*}.

Tables XV. (1) and XV. (2) express the amount of the elastic yieldings after first reversals, the amplitude being 10.

The value corresponding to $n=0$ is the amount of residual twist at the instant when all the couple is just withdrawn.

n	$\log_{10}\frac{\Gamma\{2A-n+1\}}{[\Gamma\{A-n+1\}]^2}$
9	7.601
8	8.078
7	8.238
6	8.180
5	7.958
4	7.606
3	7.146
2	6.595
1	5.966
0	5.267
−1	4.506
−2	3.690
−3	2.824
−4	1.912
−5	0.958
−6	−0.036
−7	−1.065
−8	−2.129
−9	−3.224
−10	−4.349
−11	−5.502
−12	−6.680
−13	−7.886
−14	−9.115
−15	−10.367
−16	−11.640
−17	−12.935
−18	−14.250
−19	−15.583
−20	−16.935
−21	−18.306
−22	−19.692
−23	−21.096
−24	−22.515
−25	−23.950
−26	−25.400
−27	−26.864
−28	−28.343
−29	−29.837
−30	−31.340

TABLE XV. (2). {*Hysteresis Function*}.

n	$\log_{10}\dfrac{\Gamma\{2\mathfrak{A}-n+1\}}{[\Gamma\{\mathfrak{A}-n+1\}]^2}$	n	$\log_{10}\dfrac{\Gamma\{2A-n+1\}}{[\Gamma\{\mathfrak{A}-n+1\}]^2}$
−31	−33.058	−56	−74.197
−32	−34.388	−57	−75.962
−33	−35.931	−58	−77.735
−34	−37.486	−59	−79.515
−35	−39.052	−60	−81.302
−36	−40.629	−61	−83.096
−37	−42.217	−62	−84.897
−38	−43.817	−63	−86.705
−39	−45.426	−64	−88.519
−40	−47.046	−65	−90.239
−41	−48.676	−66	−92.167
−42	−50.315	−67	−94.000
−43	−51.965	−68	−95.840
−44	−53.624	−69	−97.685
−45	−55.291	−70	−99.537
−46	−56.968	−71	−101.395
−47	−58.653	−72	−103.259
−48	−60.348	−73	−105.129
−49	−62.051	−74	−107.005
−50	−63.762	−75	−108.866
−51	−65.481	−76	−110.772
−52	−67.209	−77	−112.665
−53	−68.944	−78	−114.562
−54	−70.688	−79	−116.465
−55	−72.438	−80	−118.374

TABLE XVI. (1). {*Hysteresis Function*}.

Tables XVI. (1) and XVI. (2) express the amount of the elastic yielding after second reversals, the amplitude being ± 10.

The value corresponding to $p=0$ is the residual twist surviving the couple after one cycle of twisting and untwisting.

p	$\log_{10} \dfrac{\Gamma\{4\mathfrak{A}+p+1\}[\Gamma\mathfrak{A}+\{p+1\}]^2}{[\Gamma\{3\mathfrak{A}+p+1\}]^2}$
−9	−5.502
−8	−6.059
−7	−6.330
−6	−6.355
−5	−6.209
−4	−6.026
−3	−5.530
−2	−5.039
−1	−4.472
0	−3.825

p	$\log_{10} \dfrac{\Gamma\{4\mathfrak{A}=p=1\}[\Gamma\{\mathfrak{A}+p+1\}]^2}{[\Gamma\{3\mathfrak{A}=p=1\}]^2}$
1	−3.103
2	−2.332
3	−1.508
4	−0.635
5	0.282
6	1.241
7	2.237
8	3.270
9	4.335
10	5.432
11	6.558
12	7.713
13	8.894
14	10.099
15	11.329
16	12.584
17	13.857
18	15.151
19	16.467
20	17.801

TABLE XVI. (2). {*Hysteresis Function*}.

p	$\log_{10}\dfrac{\Gamma\{4\mathfrak{A}+p+1\}[\Gamma\{\mathfrak{A}+p+1\}]^2}{[\Gamma\{3\mathfrak{A}+p+1\}]^2}$	p	$\log_{10}\dfrac{\Gamma\{4\mathfrak{A}+p+1\}[\Gamma\{\mathfrak{A}+p+1\}]^2}{[\Gamma\{3\mathfrak{A}+p+1\}]^2}$
21	19.154	41	49.285
22	20.525	42	50.916
23	21.912	43	52.557
24	23.316	44	54.208
25	24.737	45	55.868
26	26.173	46	57.537
27	27.624	47	59.215
28	29.089	48	60.902
29	30.568	49	62.599
30	32.061	50	64.303
31	33.568	51	66.016
32	35.086	52	67.737
33	36.618	53	69.466
34	38.161	54	71.202
35	39.717	55	72.947
36	41.284	56	74.700
37	42.863	57	76.460
38	44.453	58	78.227
39	46.053	59	80.002
40	47.664	60	81.783

TABLE XVII. *{Hysteresis Function}.*

n	$\log_{10}\dfrac{\Gamma\{6\mathfrak{A}(-n+1)\}[\Gamma\{3\mathfrak{A}(-n+1)\}]^2}{[\Gamma\{5\mathfrak{A}(-n+1)\}]^2[\Gamma\{\mathfrak{A}(-n+1)\}]^2}$	n	$\log_{10}\dfrac{\{\Gamma 6\mathfrak{A}(-n+1)\}[\Gamma\{3\mathfrak{A}(-n+1)\}]^2}{[\Gamma\{5\mathfrak{A}(-n+1)\}]^2[\Gamma\{\mathfrak{A}(-n+1)\}]^2}$
9	6.558	−16	−11.927
8	7.111	−17	−13.211
7	7.338	−18	−14.515
6	7.339	−19	−15.840
5	7.171	−20	−17.183
4	6.869	−21	−18.540
3	6.452	−22	−19.936
2	5.940	−23	−21.320
1	5.347	−24	−22.732
0	4.681	−25	−24.160
−1	3.952	−26	−25.606
−2	3.163	−27	−27.062
−3	2.323	−28	−28.535
−4	1.435	−29	−30.020
−5	0.504	−30	−31.520
−6	−0.468	−31	−33.033
−7	−1.478	−32	−34.558
−8	−2.524	−33	−36.096
−9	−3.602	−34	−37.647
−10	−4.711	−35	−39.208
−11	−5 849	−36	−40.781
−12	−7.016	−37	−42.365
−13	−8.207	−38	−43.961
−14	−9.424	−39	−45.566
−15	−10.664	−40	−47.183

TABLE XVIII. {*Hysteresis Function*}.

p	$\log_{10}\dfrac{\Gamma\{8\mathfrak{A}+p+1\}[\Gamma\{5\mathfrak{A}+p+1\}]^2[\Gamma\{\mathfrak{A}+p+1\}]^2}{[\Gamma\{7\mathfrak{A}+p+1\}]^2[\Gamma\{3\mathfrak{A}+p+1\}]^2}$
−9	−5.849
−8	−6.414
−7	−6.651
−6	−6.664
−5	−6.506
−4	−6.212
−3	−5.806
−2	−5.304
−1	−4.720
0	−4.063
1	−3.338
2	−2.575
3	−1.731
4	−0.841
5	0.073
6	1.035
7	2.040
8	3.078
9	4.150
10	5.252
11	6.384
12	7.544
13	8.729
14	9.938
15	11.173
16	12.430
17	13.709
18	15.007
19	16.327
20	17.664

Tables XVII. and XVIII. express the yielding after third, fourth, and fifth reversals.

In Pl. XXVI, the first branch starting from the origin corresponds to TABLE XIV, second branch to T. XV, third branch to T. XVI, etc. etc.

n	$\log_{10}\dfrac{\Gamma\{10\mathfrak{A}-n+1\}[\Gamma\{7\mathfrak{A}-n+1\}]^2[\Gamma\{3\mathfrak{A}-n+1\}]^2}{[\Gamma\{9\mathfrak{A}-n+1\}]^2[\Gamma\{5\mathfrak{A}-n+1\}]^2[\Gamma\{\mathfrak{A}-n+1\}]^2}$
9	6.384
8	6.942
7	7.173
6	7.178
5	7.015
4	6.715
3	6.304
2	5.796
1	5.207
0	4.544

LIST OF PLATES.

Remarks. Unit of the couple $=6.712\times10^6$ c.g.s. unit; it is denoted by $\mathfrak{C}$.

Unit of the twist $=1.845\times10^{-3}$ radians; it is denoted by τ.

Unit of the time = one minute; it is denoted by t.

Unit of the temperature = one centigrade; it is denoted by T.

Pl. I.

Fig. 1. Preliminary experiment, on sandstone, shows great deviation from Hooke's law and the existence of torsional hysteresis.

Pl. II.

Fig. 2. Front-view of the twisting apparatus.

Fig. 3. Side-view of the twisting apparatus.

Fig. 4. Plan of the whole arrangement.

Fig. 5. Frame-work carrying the mirror.

Pl. III.

Fig. 6. Curve A. Yielding of the support.

Curve B. Twist of specimen No. 12_1.

They show that the result of observation is not disturved by the yielding of the support.

Pls. IV. and V.

Figs. 7. and 8. Effect of cyclical application of positive and negative couples, gradually increasing in their absolute amount. They show the existence of torsional hysteresis, even in the case where Hooke's law holds tolerably good. Specimens No. 32_1 and 8_2.

Pl. VI.

Fig. 9. Relation between the negative couple required to annihilate the residual twist and the original couple. Deduced from the observations in Figs. 7 and 8.

Fig. 23. Relation between the residual twist and the amplitude—i.e. maximum amount of the applied couple.

Fig. 24. Relation between the modulus of rigidity and the amplitude in the specimens No. 32_1 and 8_2.

Pl. VII.

Fig. 10. Elastic yielding of specimen No. 3_2 under constant couple.

Figs. 42 and 43. Curve of the Elastic Recovery. The specimen, No. 4_1, was subjected to the twisting couple, $M_0=2000$ and $M=1500$, during a week and then it was released from the couple; i.e. $M_0=2000$ and $M=0$.

Fig. 53. Theoretical curve for Elastic Recovery.

Pl. VIII.

Fig. 11. Elastic Yielding of specimen No. 4_1 under several constant couples.

Fig. 14. Theoretical curves for Elastic Yielding.

Pl. IX.

Figs. 12 and 13. Relation between the rate of elastic yielding and time. These are deduced from the observations given in Fig. 11, Pl. VIII; the specimen emploied being sandstone. Full lines are theoretical curves.

Pl. X.

Figs. 15-18. Elastic Yielding after long time. Specimen No. 4_1.

Pl. XI.

Figs. 19-21. In each figure, the upper curve shows the variation of temperature with time in the laboratory, while the lower curve shows the variation of the amount of twist in corresponding time. Specimen No. 4_1.

Fig. 22. Relation between the change of the amount of twist and the temperature-variation. This is deduced from those in Figs. 19–21.

Pl. XII.

Figs. 25 and 26. In these figures, each series of observations admits of being connected by a straight line, so that Hooke's law holds tolerably good. The difference of inclinations, however, shows that the modulus of rigidity never remains constant. These observations were made on one and the same specimen; i.e. No. 4_2. Thus, approximate comformity to Hooke's law is no proof for non-existence of hysteresis.

Pls. XIII.–XVII.

Figs. 27–41. Examples of torsional hysteresis in several rocks of different kinds.

Specimens: No. 3_3 ($M_0=1000$); 3_2; 3_1; 5_2; 6_1; 6_2; 10_1; 9_1; 8_1; 7_2; 31_2; 18_1; 17_2; 3_3 ($M_0=2000$); and 3 ($M_0=800$).

Pl. XVIII.

Fig. 44. Effect of the elastic recovery on the cycles. The specimen, No. 3_3, was subjected under the twisting couple, $M_0=2000$, $M=800$, during 306.5 hours and then taking that strained state for the centre of symmetry of the cyclic process, it was twisted to and fro.

Pl. XIX.

Fig. 45. Twisting and untwisting, the centre of symmetry being situated at a twisted state.

Pl. XX.

Fig. 46. This shows that the modulus of rigidity diminishes when the amplitude of the cycle is increased, but it increases when the centre of symmetry of the cyclic process is deviated from neutral state.

Pl. XXI.

Fig. 47. Effect of the time on torsional hysteresis. Specimen No. 14_1.

Pl. XXII.

Fig. 48. Example of neutralization of a non-virgin piece. Specimen No. 16_1.

Pl. XXIII.

Fig. 49. Further example of torsional hysteresis. Specimen No. 14_1.

Pl. XXIV.

Eig. 50. Gradual diminution of the modulus of rigidity, from perfectly rigid substance to metals and then to rocks and ideal fluid. Axis of abscissa and axis of ordinate correspond to perfect rigid substance and ideal fluid respectively.

Specimen; Soft iron; Nos. 7_1; 17_2; 14_1; 2_1; 16_1; 3_1; 32_1.

Pl. XXV.

Figs. 51 and 52. Time-lag due to inertia. Theoretical curve. The moment of inertia in the former is three times smaller than that of the latter.

Pl. XXVI.

Fig. 54. Particular example of the Hysteresis-function due to the elastic yielding.

Pl. XXVII.

Figs. 55-59. Examples of the torsional hysteresis due to the elastic yielding, calculated from the Hysteresis function by giving different values to the constant involved in the function and to the part which is in conformity with Hooke's law.

In each figure, an inclined straight line represents what the curve shrinks when the yielding becomes negligibly small.

These Figs. are to be compared with those in Pls. XIV. and XV, which have been drawn from the results of observation.

LIST OF TABLES.

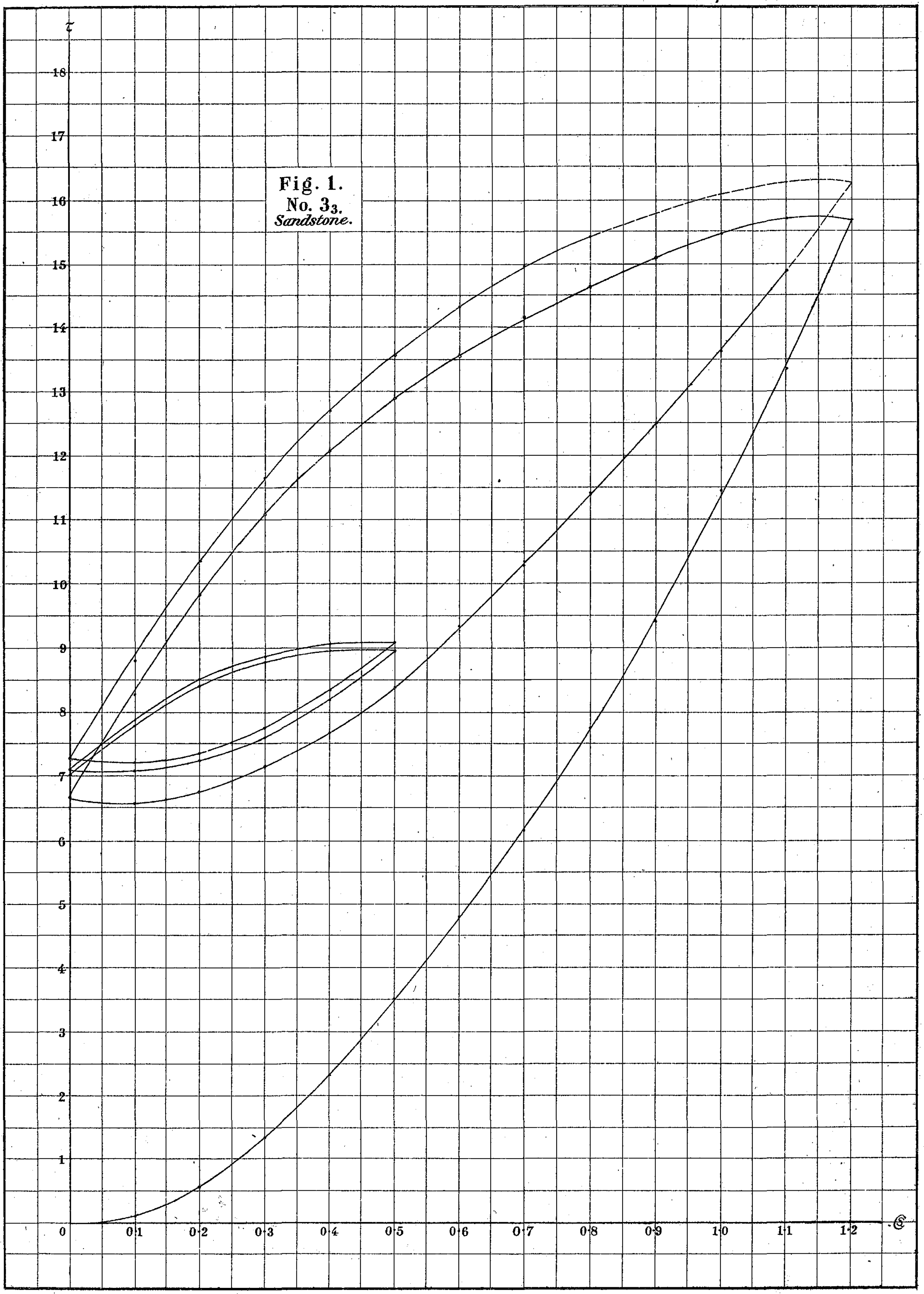
Fig. 1.
No. 3₃.
Sandstone.
τ
18
17
16
15
14
13
12
11
10
9
8
7
6
5
4
3
2
1
0
0·1
0·2
0·3
0·4
0·5
0·6
0·7
0·8
0·9
1·0
1·1
1·2
ε

Fig. 2.

Front-view

Fig. 3.

Side-view.

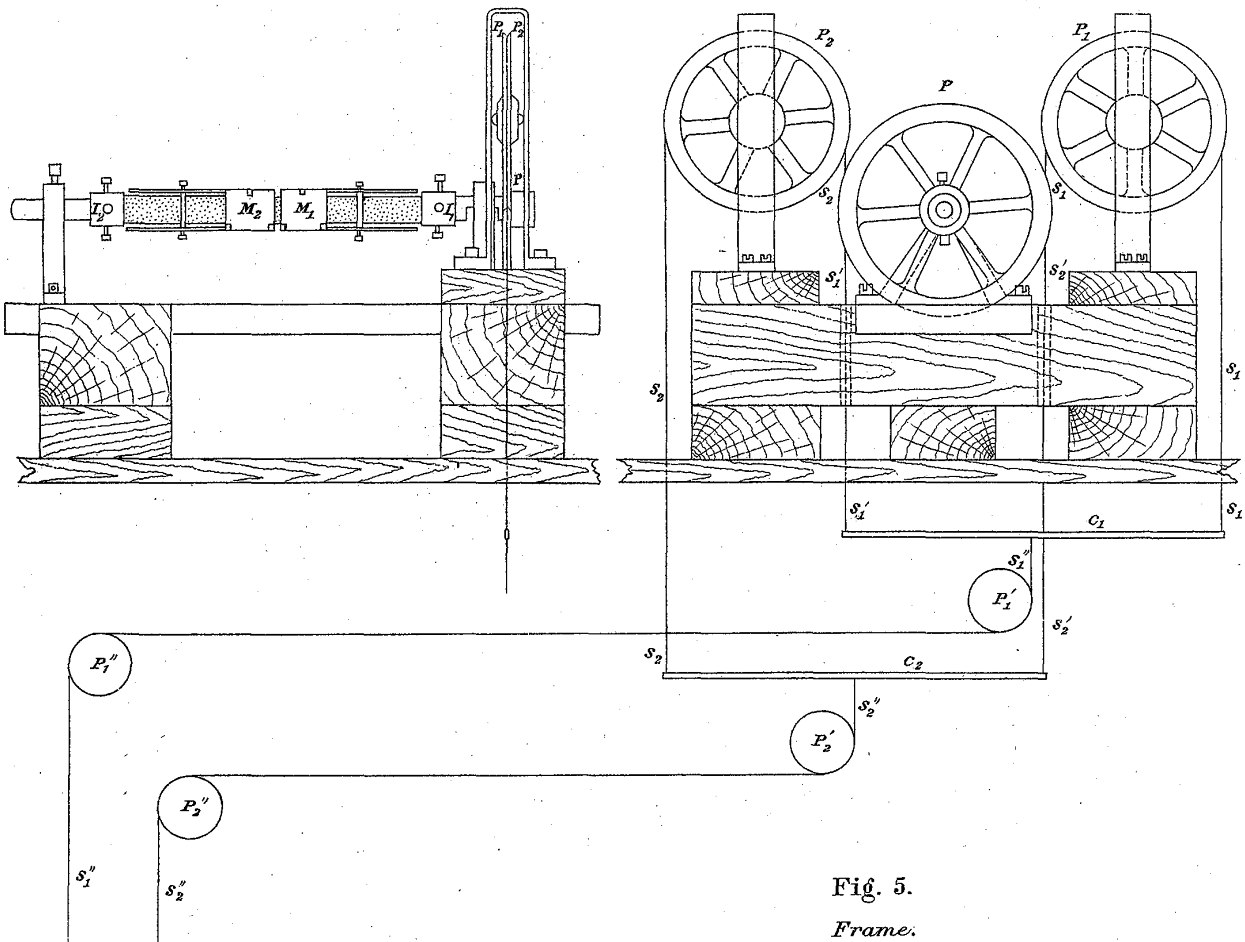

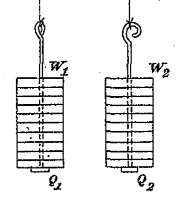

Fig. 5.

Frame.

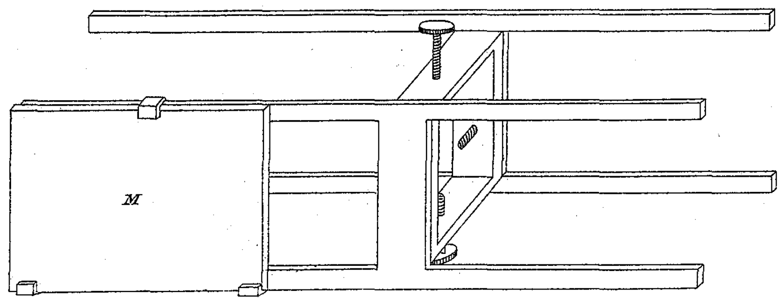

Fig. 4.

Plan of the arrangement.

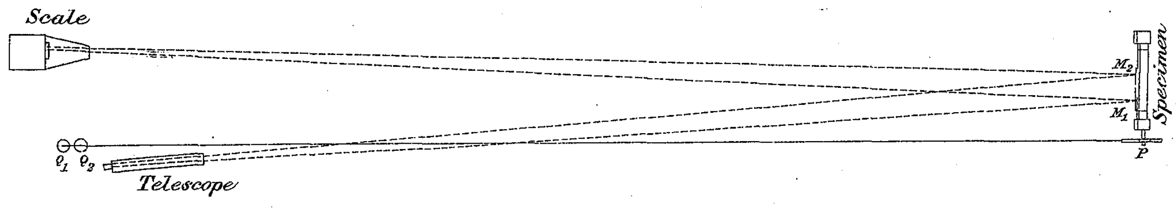

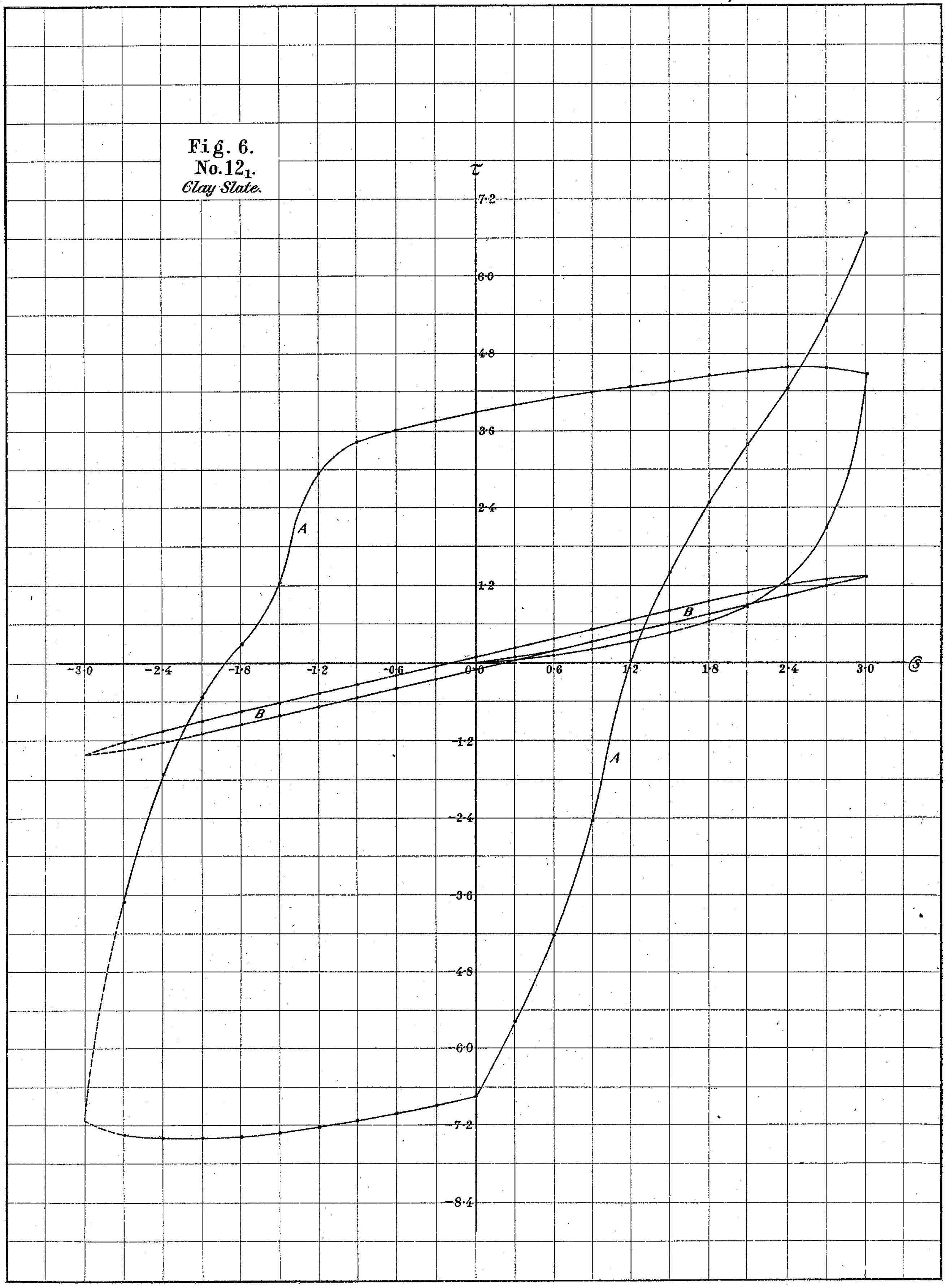
Fig. 6.
No. 12_1.
Clay Slate.
τ
7·2
6·0
4·8
3·6
2·4
1·2
-1·2
-2·4
-3·6
-4·8
-6·0
-7·2
-8·4
-3·0
-2·4
-1·8
-1·2
-0·6
0·0
0·6
1·2
1·8
2·4
3·0
A
B

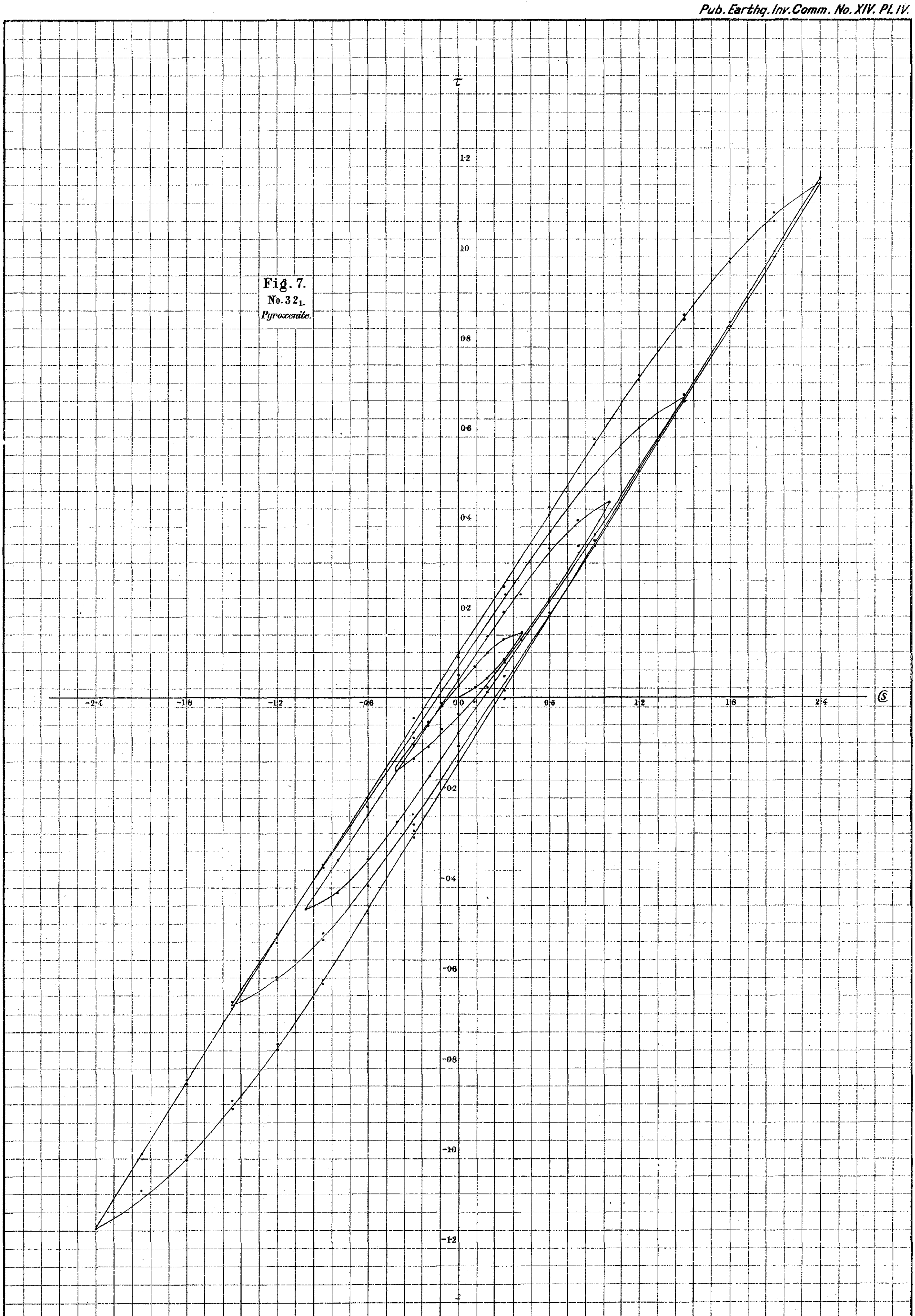
Fig. 7.
No. 3 2₁.
Pyroxenite.
τ
1·2
1·0
0·8
0·6
0·4
0·2
0·0
-0·2
-0·4
-0·6
-0·8
-1·0
-1·2
-2·4
-1·8
-1·2
-0·6
0·6
1·2
1·8
2·4
𝔖

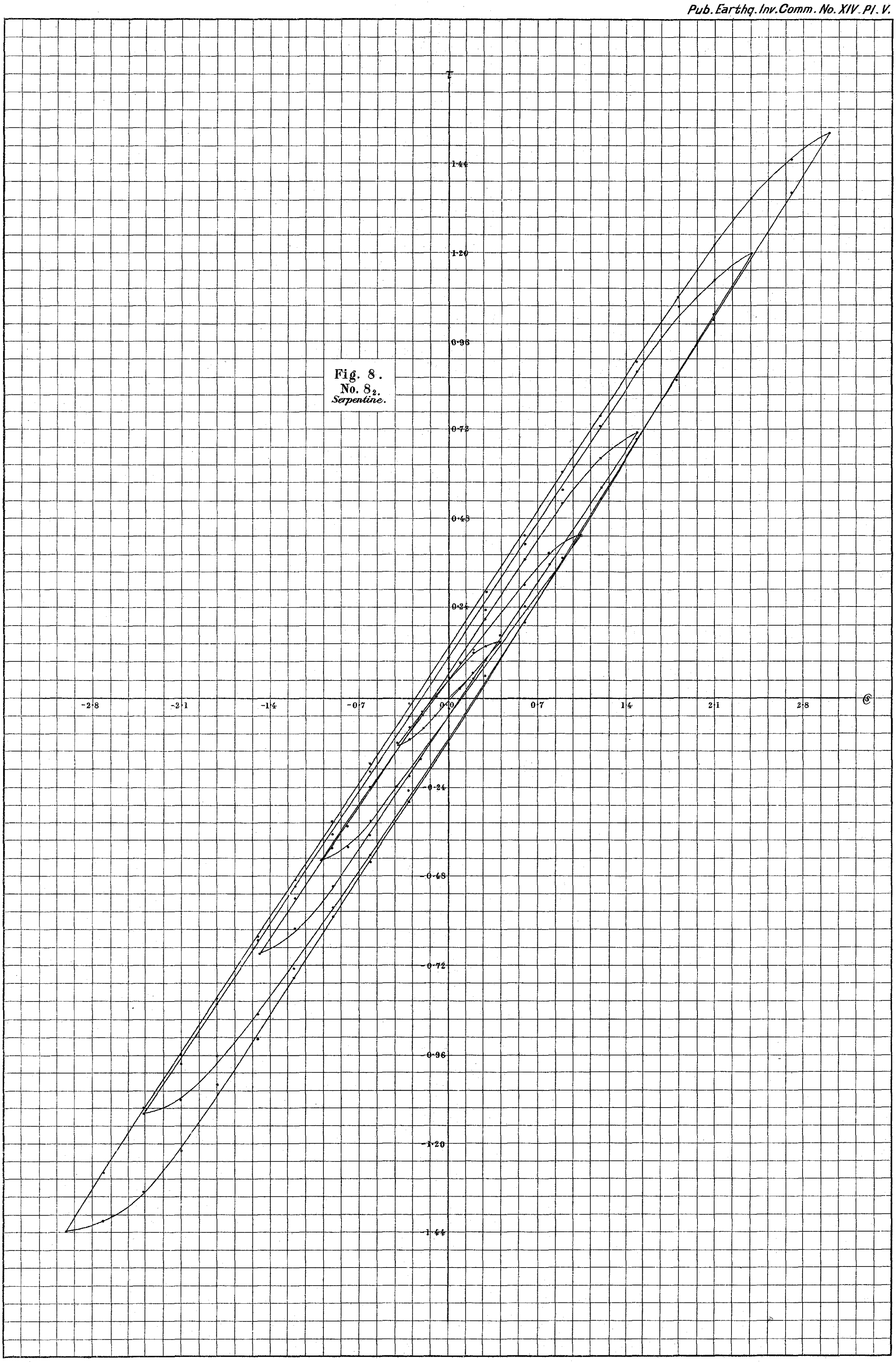

Fig. 8.
No. 8_2.
Serpentine.
1·44
1·20
0·96
0·72
0·48
0·24
-2·8
-2·1
-1·4
-0·7
0·0
0·7
1·4
2·1
2·8
-0·24
-0·48
-0·72
-0·96
-1·20
-1·44

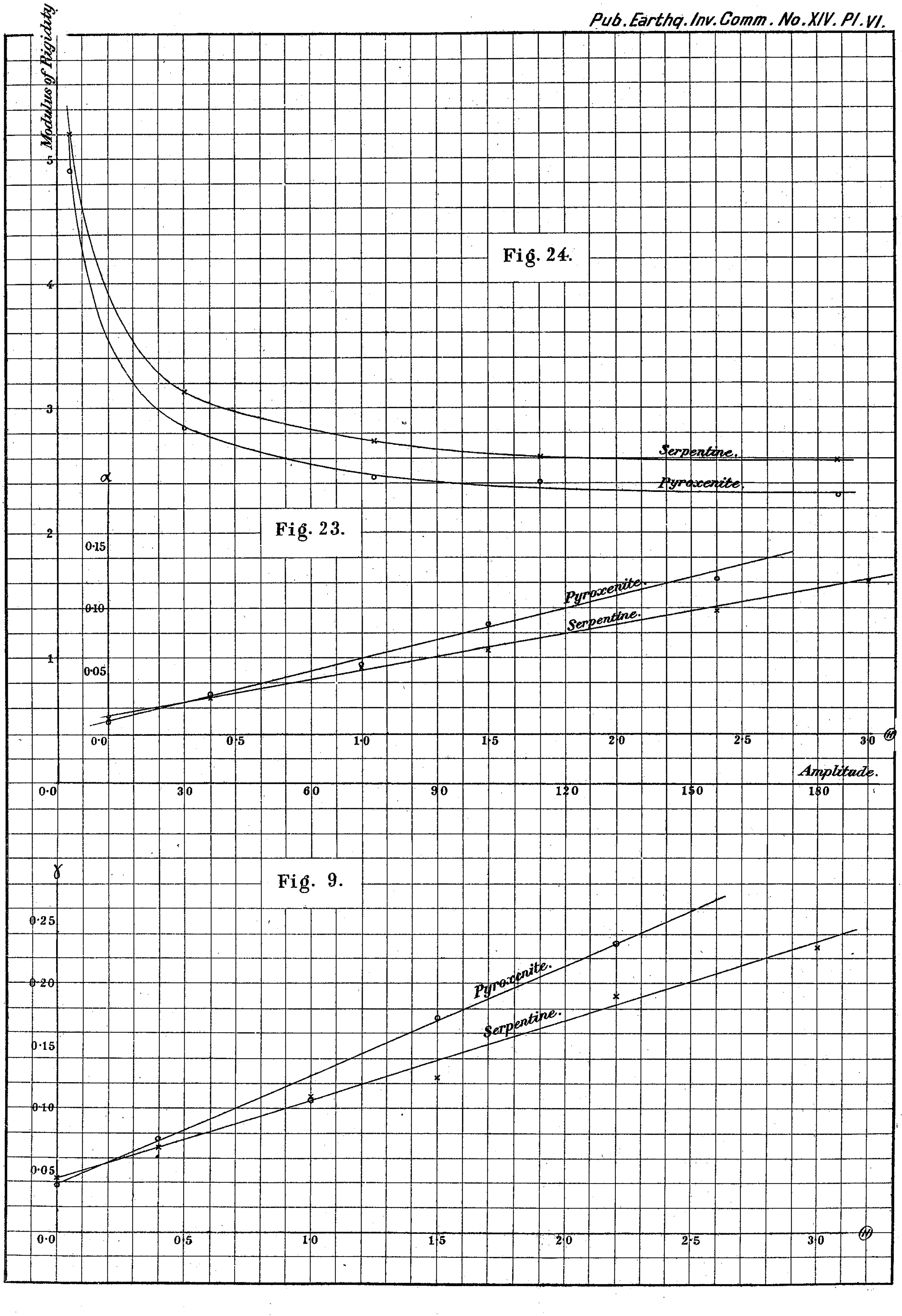
Modulus of Rigidity
Fig. 24.
Serpentine.
Pyroxenite.
α
Fig. 23.
0·15
0·10
0·05
Pyroxenite.
Serpentine.
0·0
0·5
1·0
1·5
2·0
2·5
3·0
Amplitude.
0·0
30
60
90
120
150
180
γ
Fig. 9.
0·25
0·20
0·15
0·10
0·05
Pyroxenite.
Serpentine.
0·0
0·5
1·0
1·5
2·0
2·5
3·0

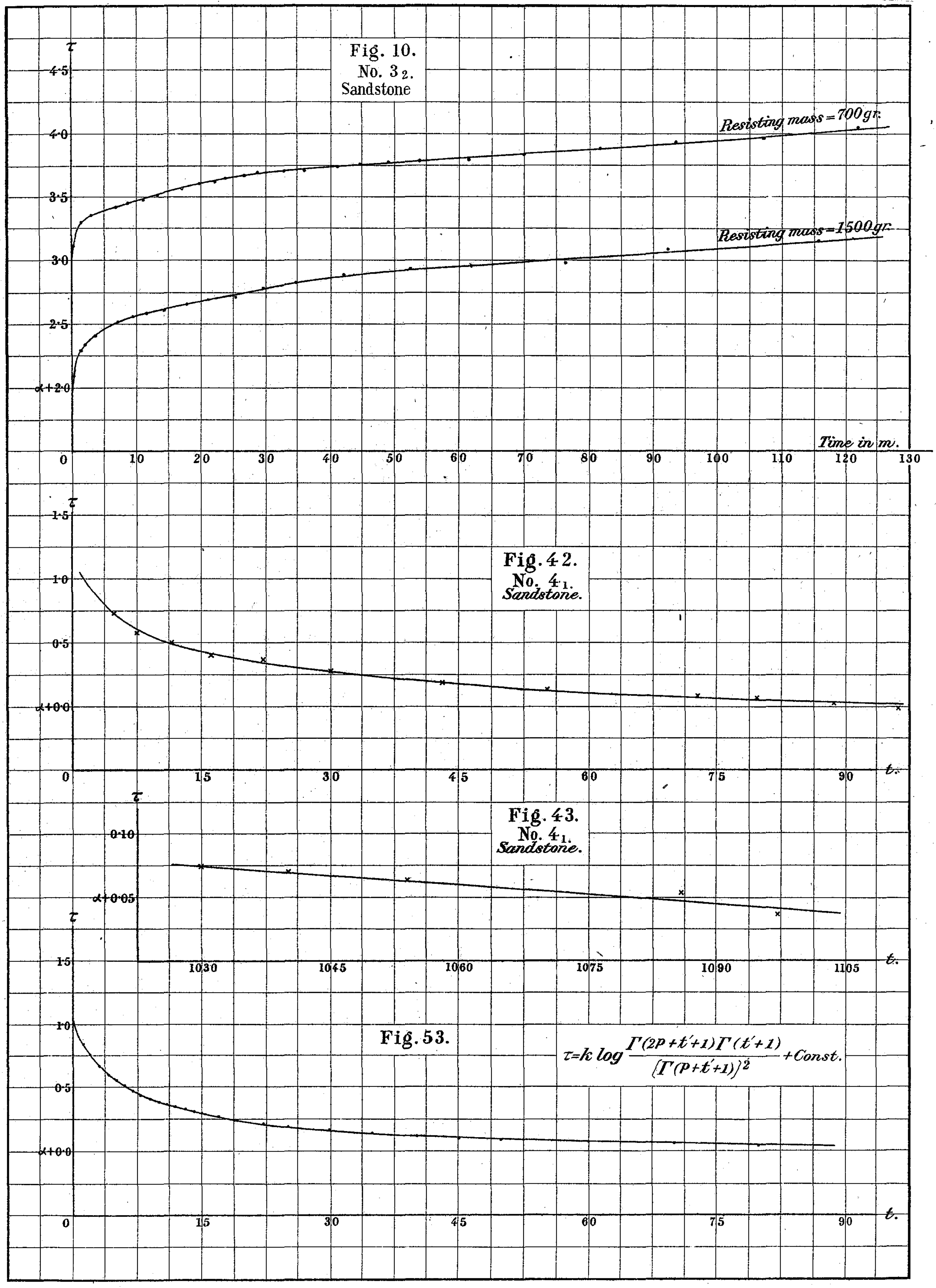
Fig. 10.
No. 3_2.
Sandstone
Resisting mass = 700 gr.
Resisting mass = 1500 gr.
Time in m.
Fig. 42.
No. 4_1.
Sandstone.
Fig. 43.
No. 4_1.
Sandstone.
Fig. 53.
$\tau = k \log \dfrac{\Gamma(2p+t'+1)\,\Gamma(t'+1)}{\{\Gamma(p+t'+1)\}^2} + Const.$

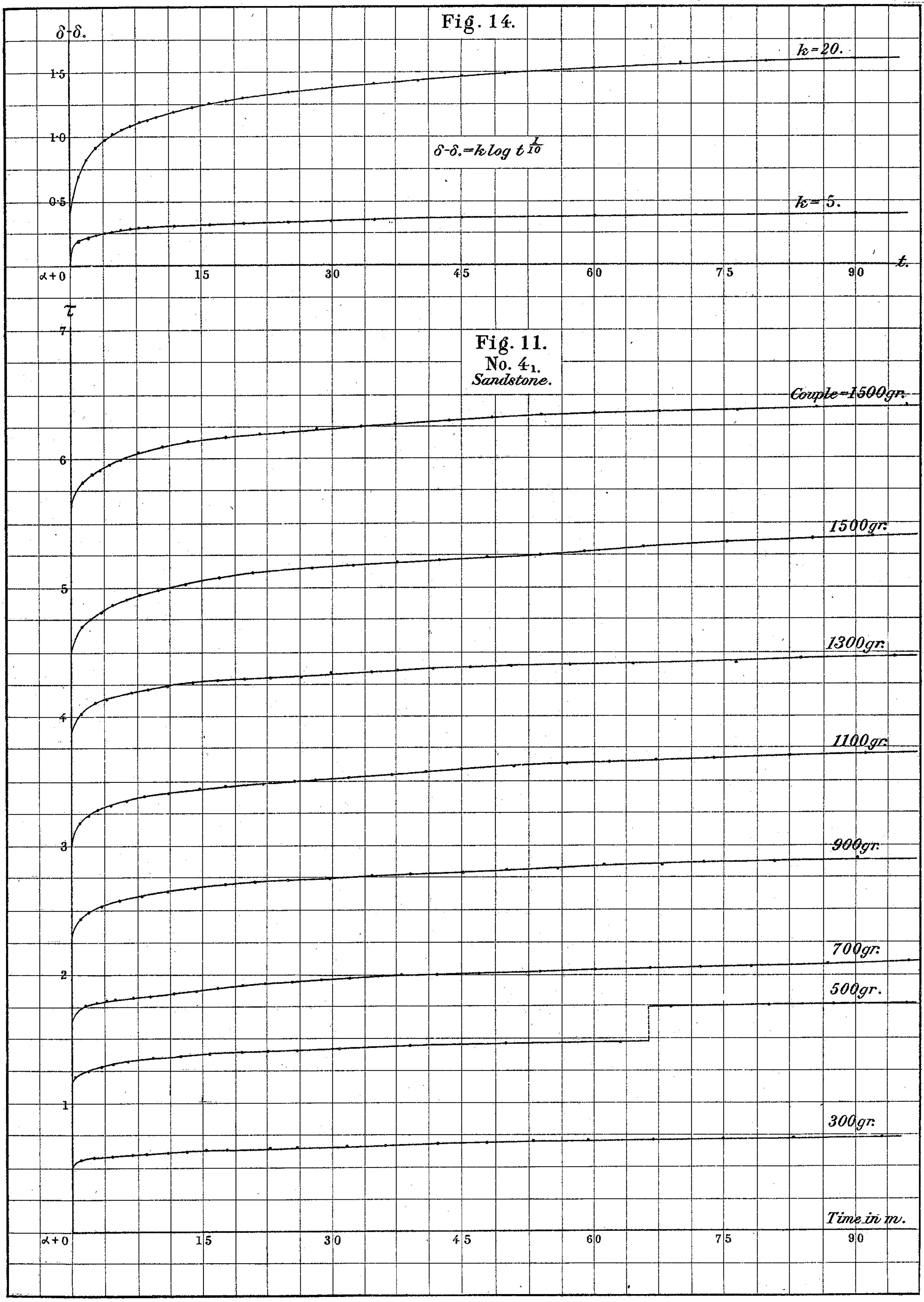
Fig. 14.
δ-δ.
1·5
1·0
0·5
α+0
15
30
45
60
75
90
t.
k=20.
k=5.
δ-δ.=k log t 1/10
Fig. 11.
No. 4₁.
Sandstone.
τ
7
6
5
4
3
2
1
Couple=1500gr.
1500gr.
1300gr.
1100gr.
900gr.
700gr.
500gr.
300gr.
Time in m.
α+0
15
30
45
60
75
90

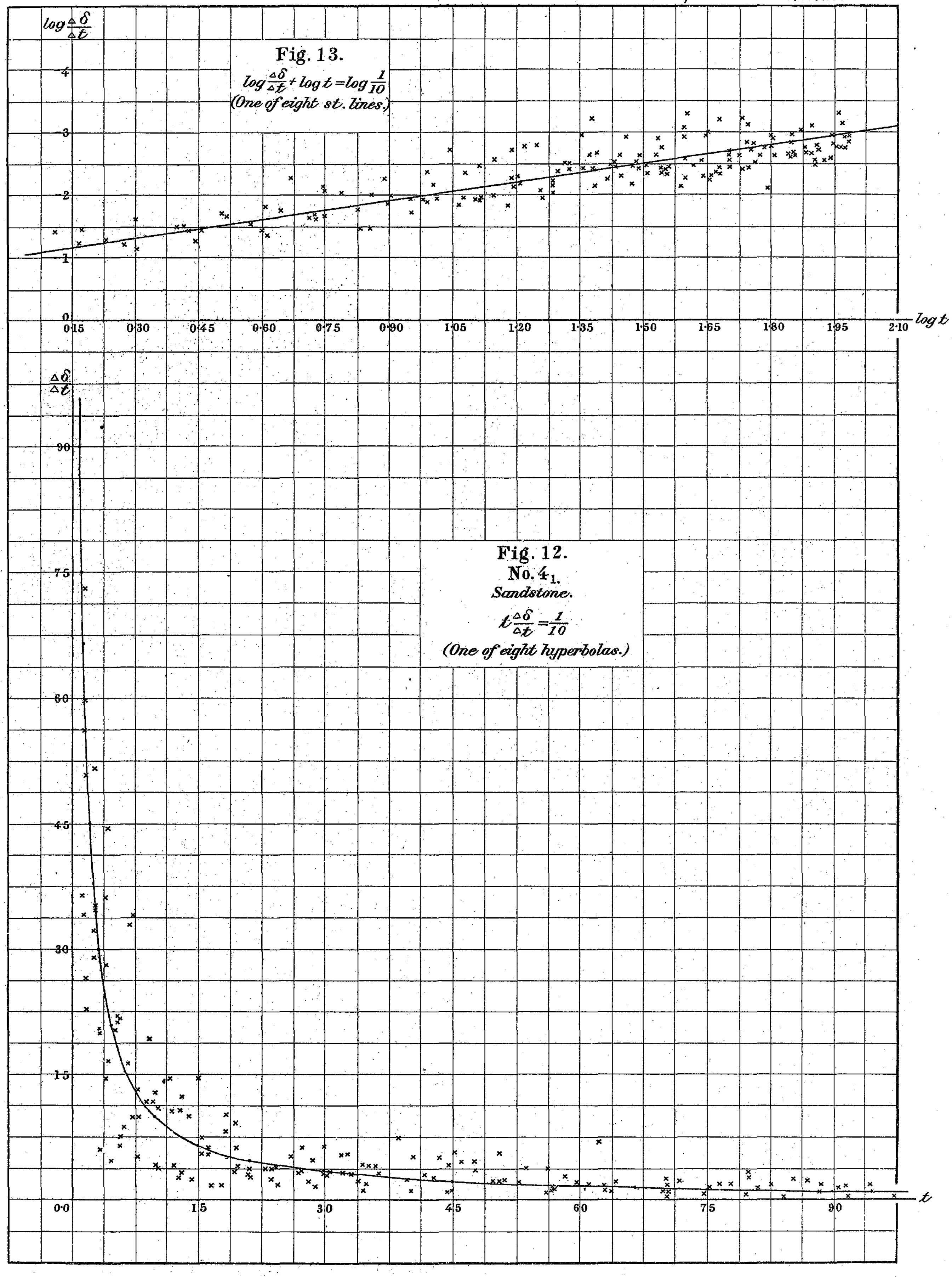

Fig. 13.
$\log\frac{\Delta\delta}{\Delta t} + \log t = \log\frac{1}{10}$
(One of eight st. lines.)
$\log\frac{\Delta\delta}{\Delta t}$
$\log t$
Fig. 12.
No. 4_1.
Sandstone.
$t\frac{\Delta\delta}{\Delta t} = \frac{1}{10}$
(One of eight hyperbolas.)
$\frac{\Delta\delta}{\Delta t}$
t

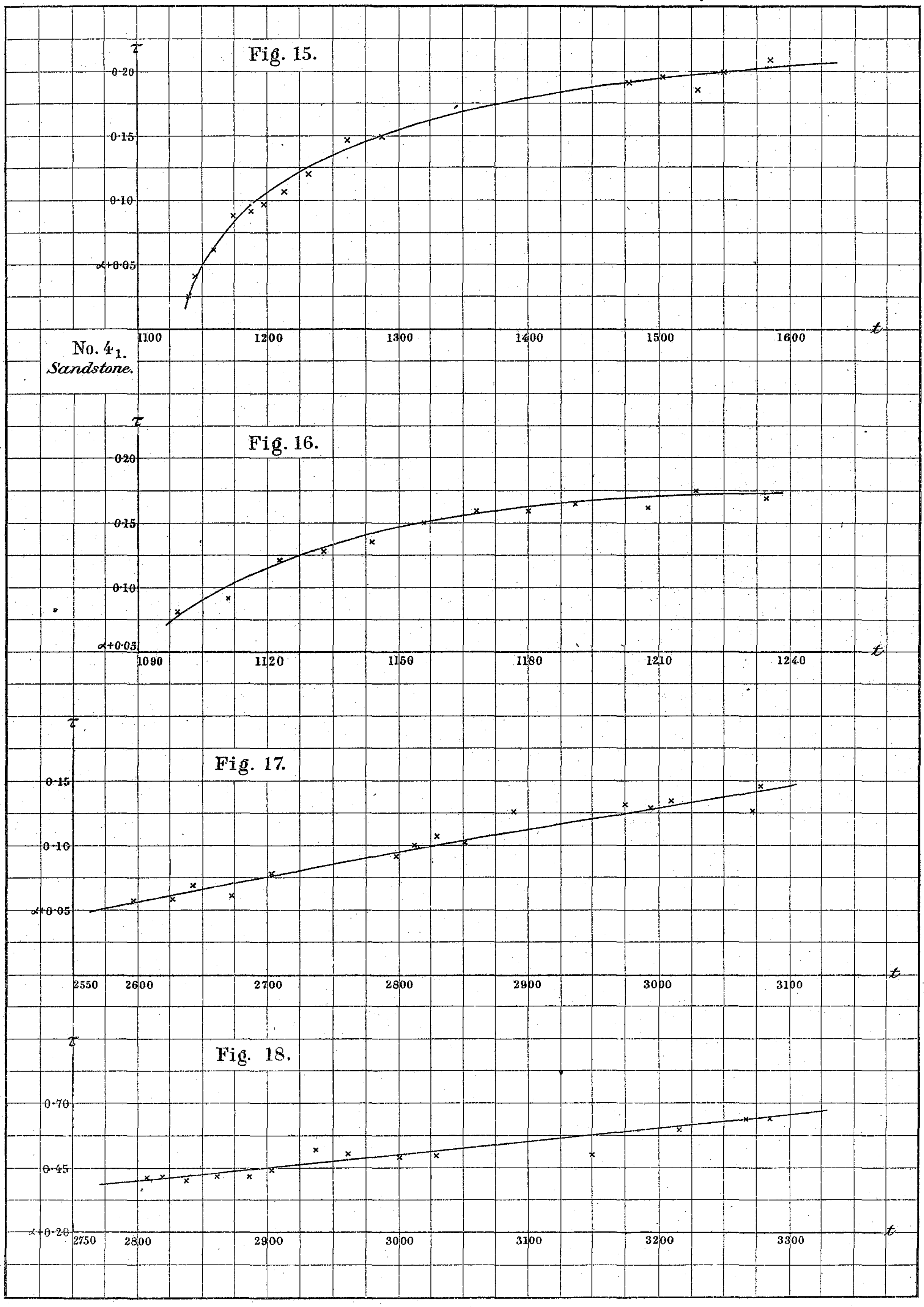
Fig. 15.
τ
0·20
0·15
0·10
α+0·05
1100
1200
1300
1400
1500
1600
t
No. 4₁.
Sandstone.
Fig. 16.
τ
0·20
0·15
0·10
α+0·05
1090
1120
1150
1180
1210
1240
t
Fig. 17.
τ
0·15
0·10
α+0·05
2550
2600
2700
2800
2900
3000
3100
t
Fig. 18.
τ
0·70
0·45
α+0·20
2750
2800
2900
3000
3100
3200
3300
t

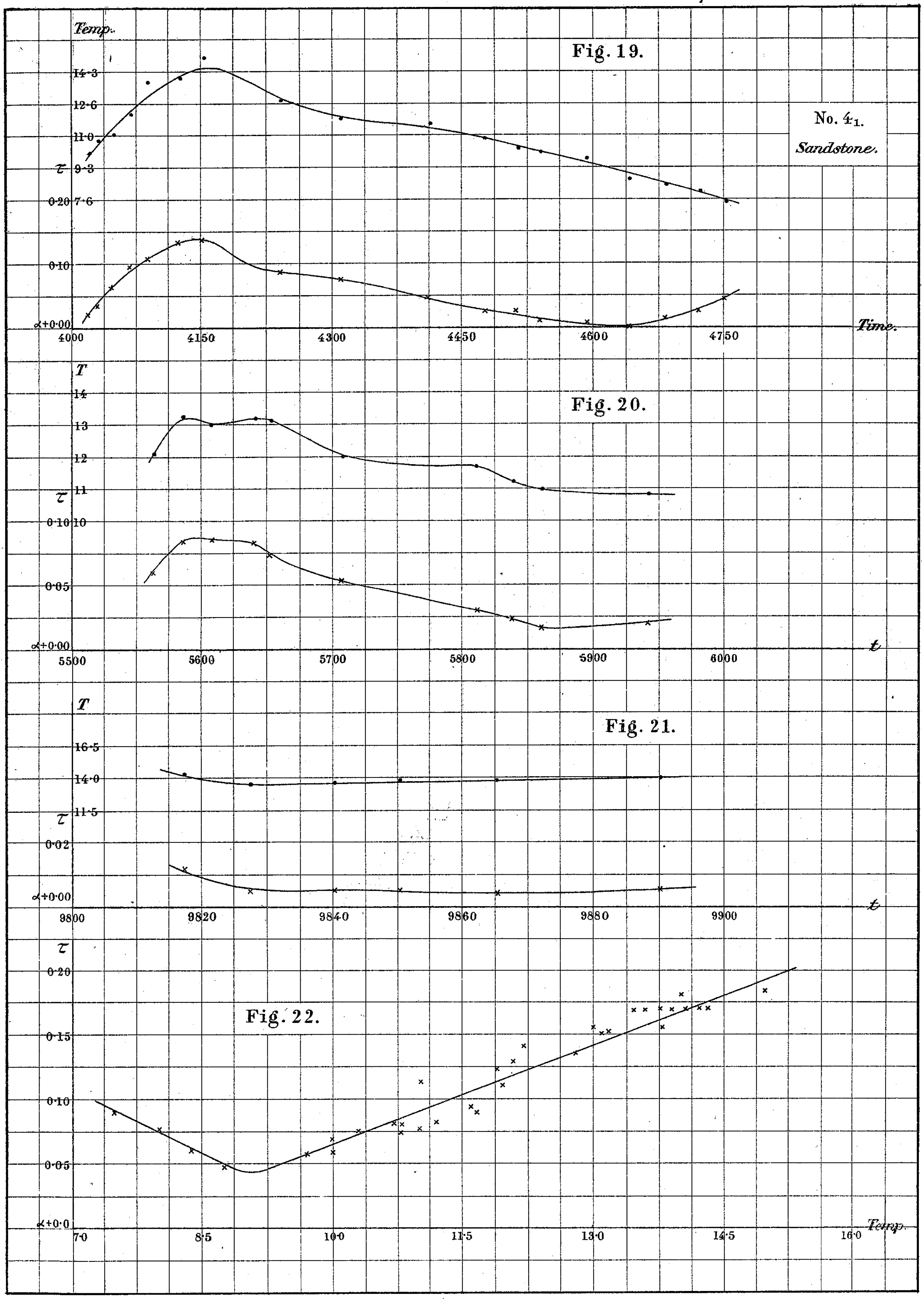
Fig. 19.
No. 41.
Sandstone.
Temp.
14·3
12·6
11·0
9·3
7·6
τ
0·20
0·10
α+0·00
4000
4150
4300
4450
4600
4750
Time.
Fig. 20.
T
14
13
12
11
10
τ
0·10
0·05
α+0·00
5500
5600
5700
5800
5900
6000
t
Fig. 21.
T
16·5
14·0
11·5
τ
0·02
α+0·00
9800
9820
9840
9860
9880
9900
t
Fig. 22.
τ
0·20
0·15
0·10
0·05
α+0·0
7·0
8·5
10·0
11·5
13·0
14·5
16·0
Temp.

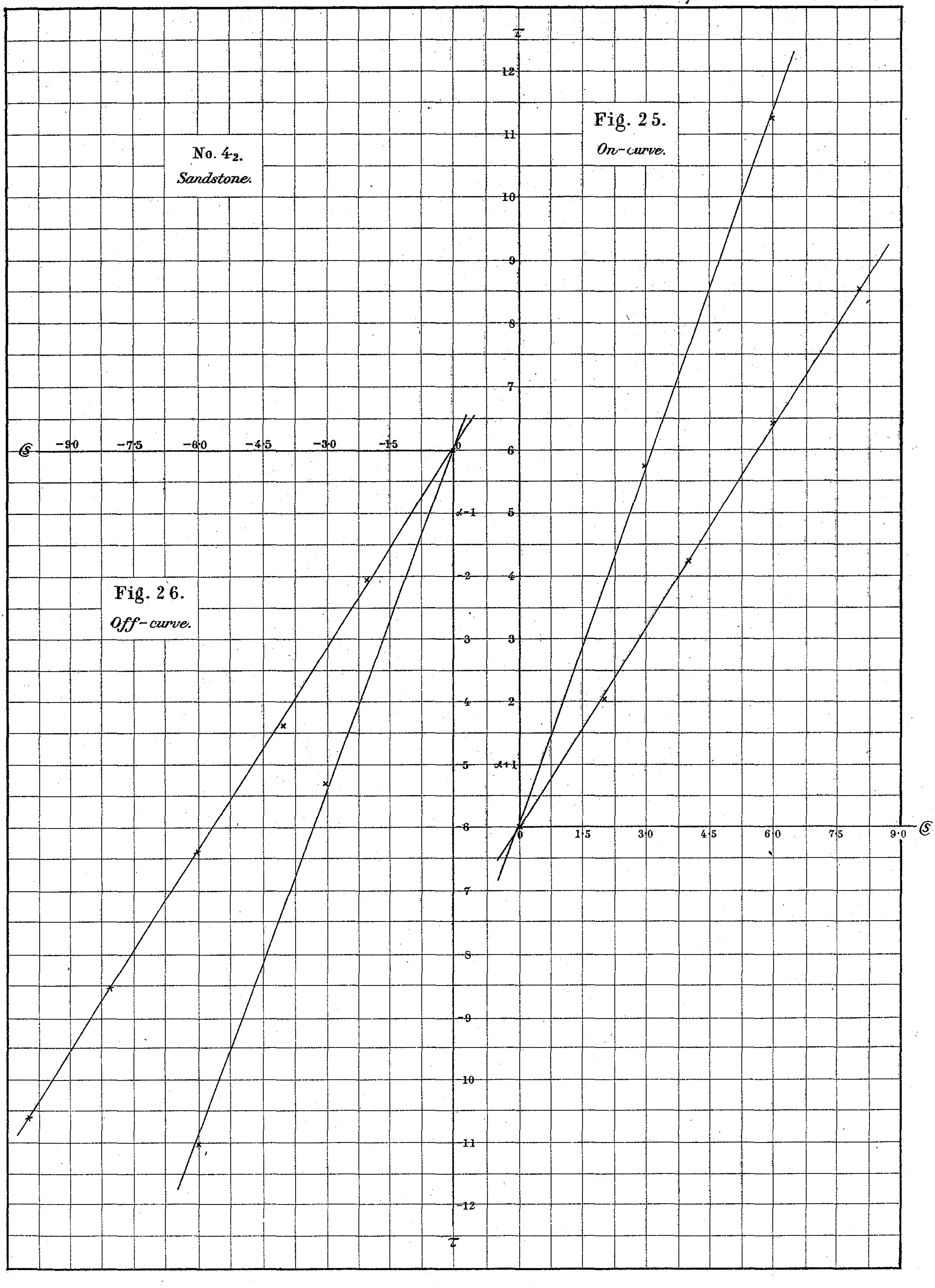
No. 4₂.
Sandstone.
Fig. 25.
On-curve.
Fig. 26.
Off-curve.
−9·0
−7·5
−6·0
−4·5
−3·0
−1·5
1·5
3·0
4·5
6·0
7·5
9·0

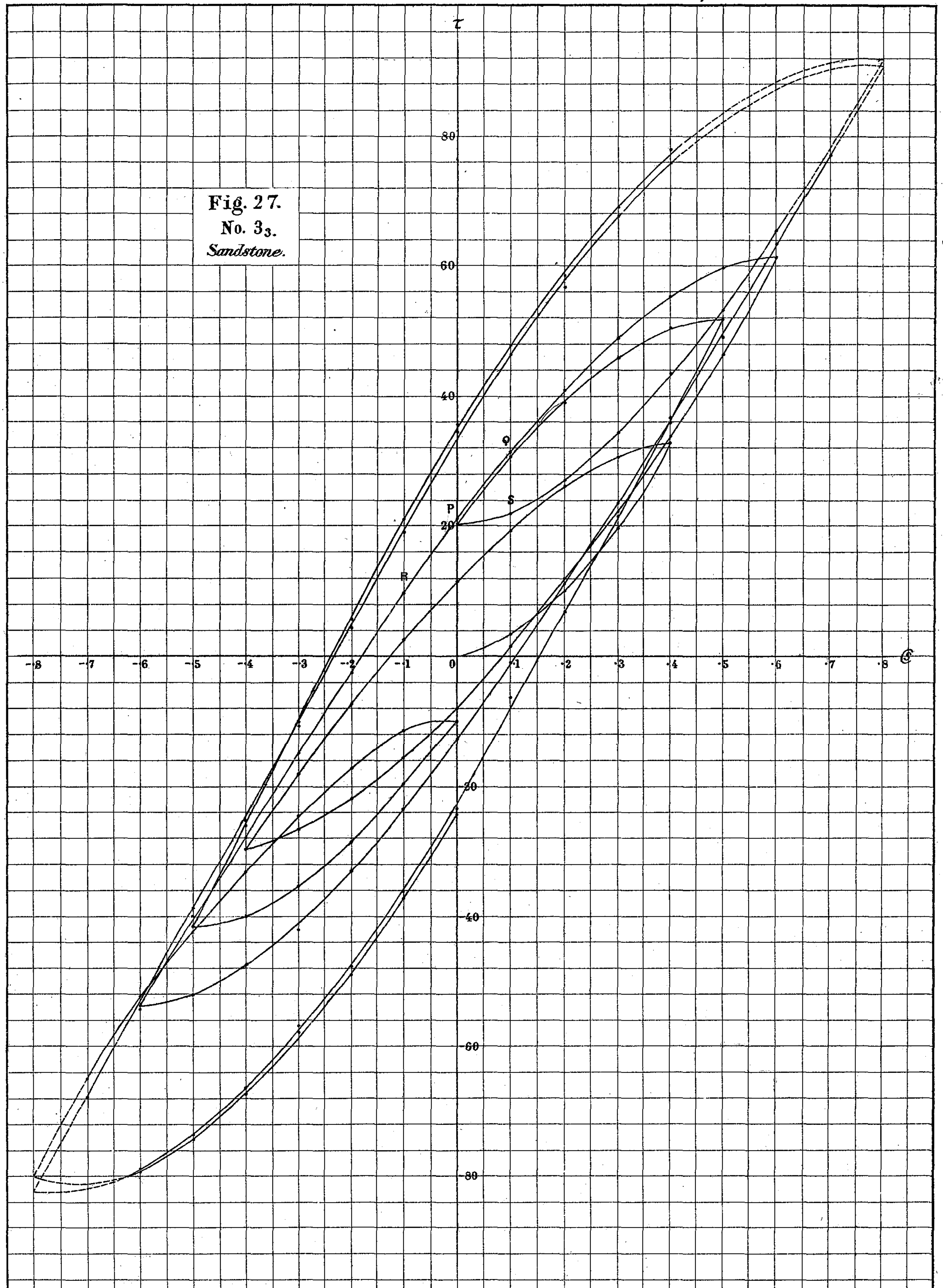

Fig. 27.
No. 3_3.
Sandstone.
τ
80
60
40
20
20
40
60
80
P
Q
R
S
·8
·7
·6
·5
·4
·3
·2
·1
0
·1
·2
·3
·4
·5
·6
·7
·8
𝔈

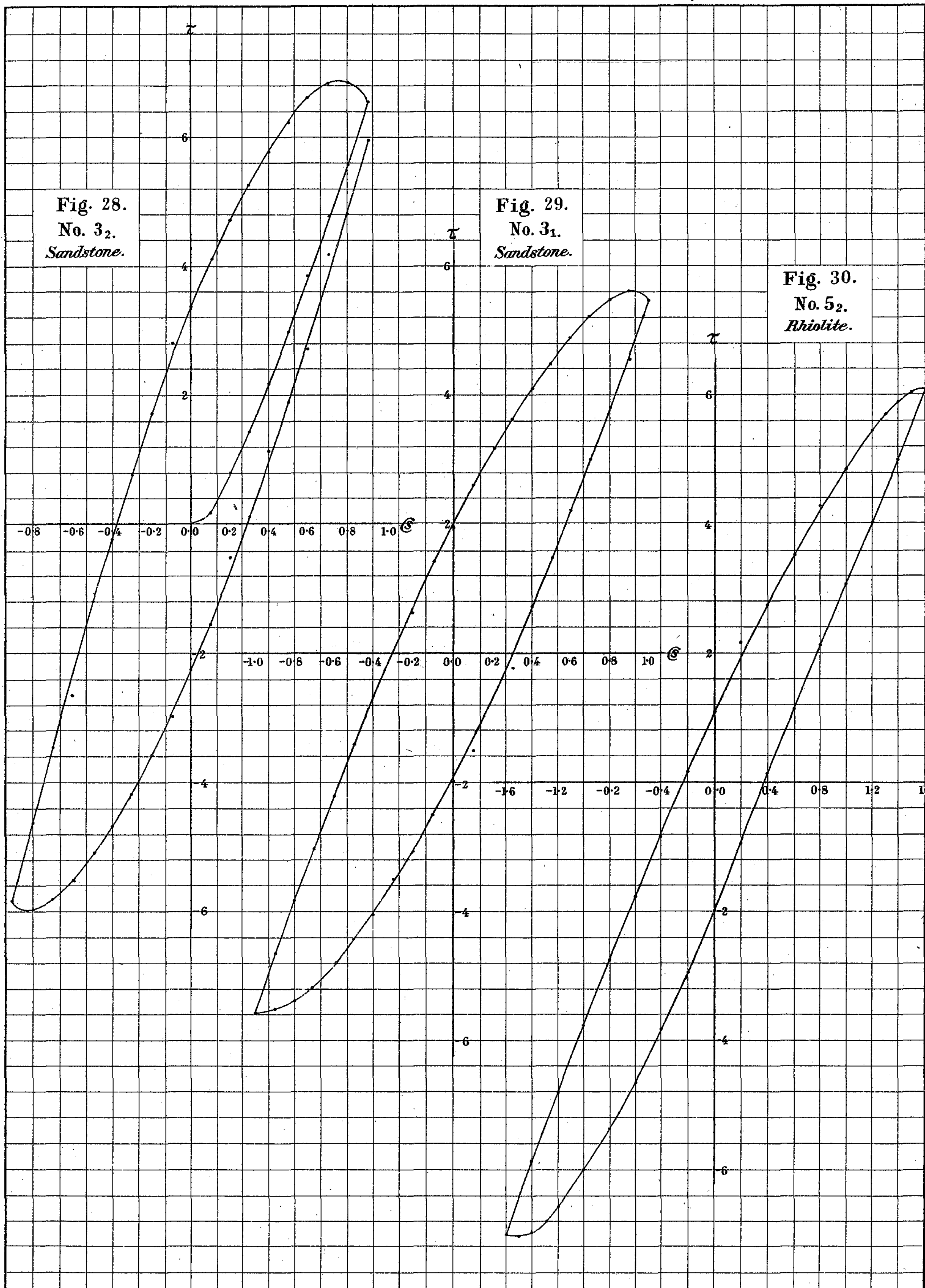
Fig. 28.
No. 3_2.
Sandstone.
Fig. 29.
No. 3_1.
Sandstone.
Fig. 30.
No. 5_2.
Rhiolite.

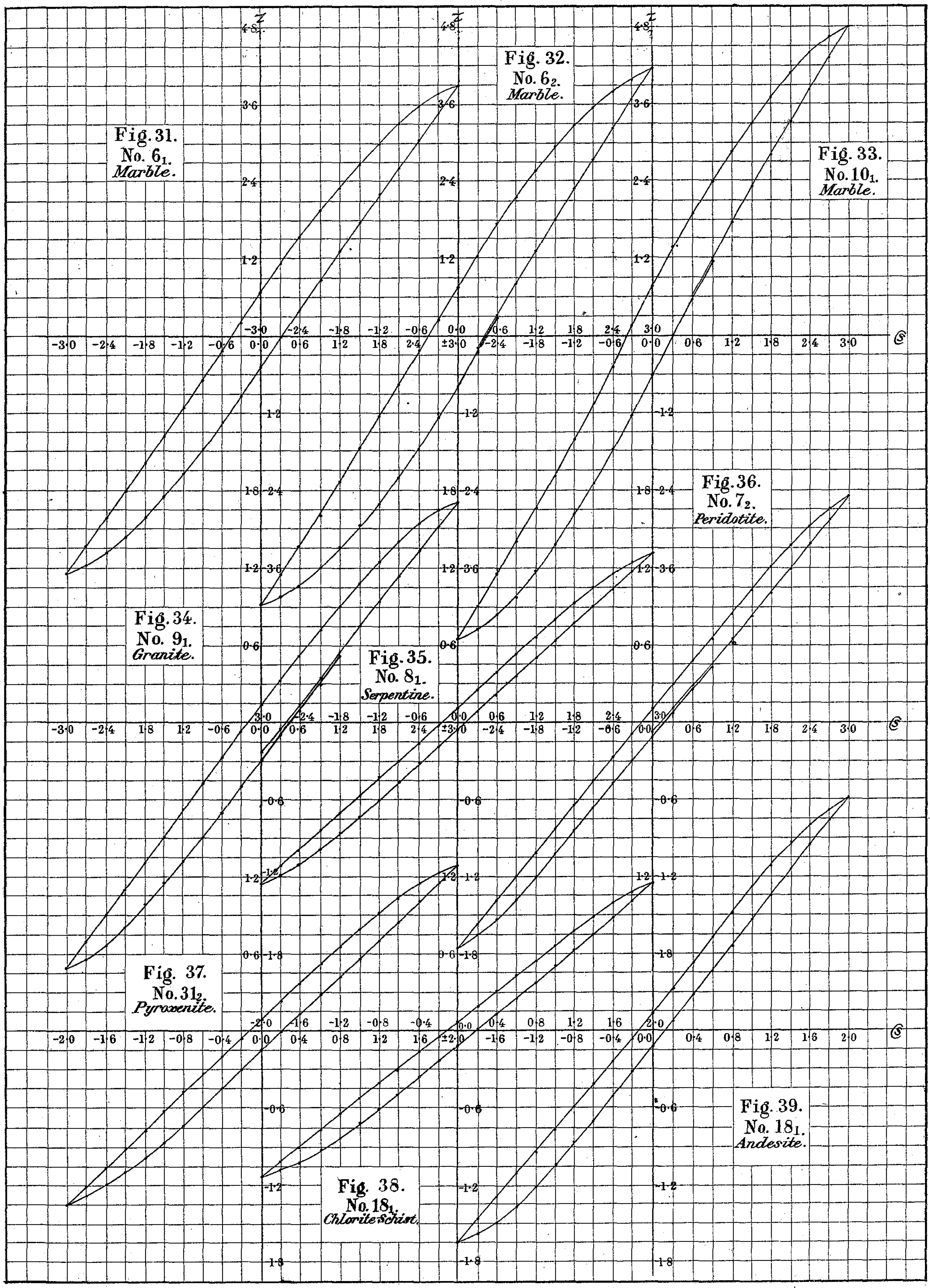
Fig. 31.
No. 6_1.
Marble.
Fig. 32.
No. 6_2.
Marble.
Fig. 33.
No. 10_1.
Marble.
Fig. 34.
No. 9_1.
Granite.
Fig. 35.
No. 8_1.
Serpentine.
Fig. 36.
No. 7_2.
Peridotite.
Fig. 37.
No. 31_2.
Pyroxenite.
Fig. 38.
No. 18_1.
Chlorite Schist.
Fig. 39.
No. 18_1.
Andesite.

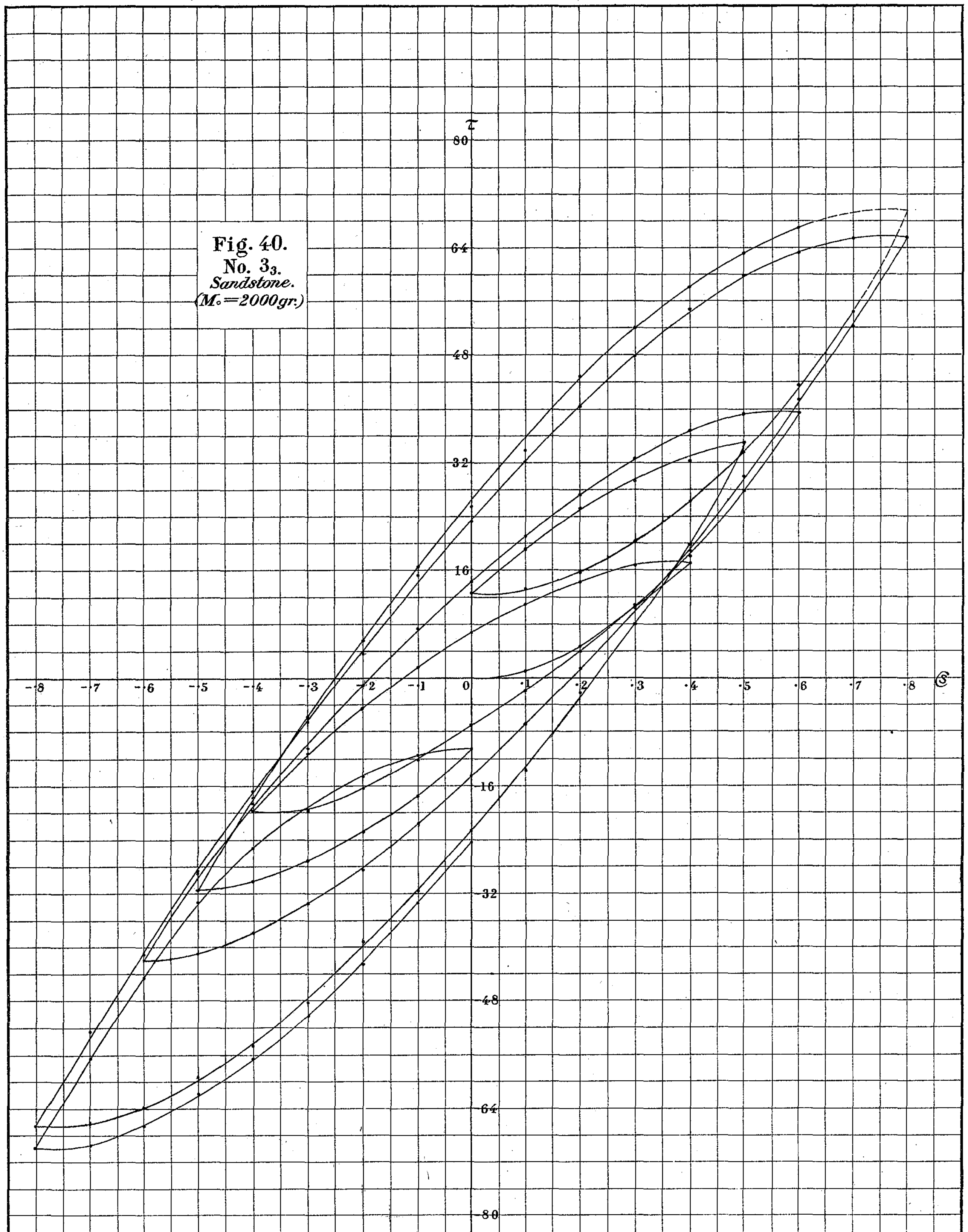
Fig. 40.
No. 3_3.
Sandstone.
(M_0=2000gr.)
τ
80
64
48
32
16
-16
-32
-48
-64
-80
-·8
-·7
-·6
-·5
-·4
-·3
-·2
-·1
0
·1
·2
·3
·4
·5
·6
·7
·8
S

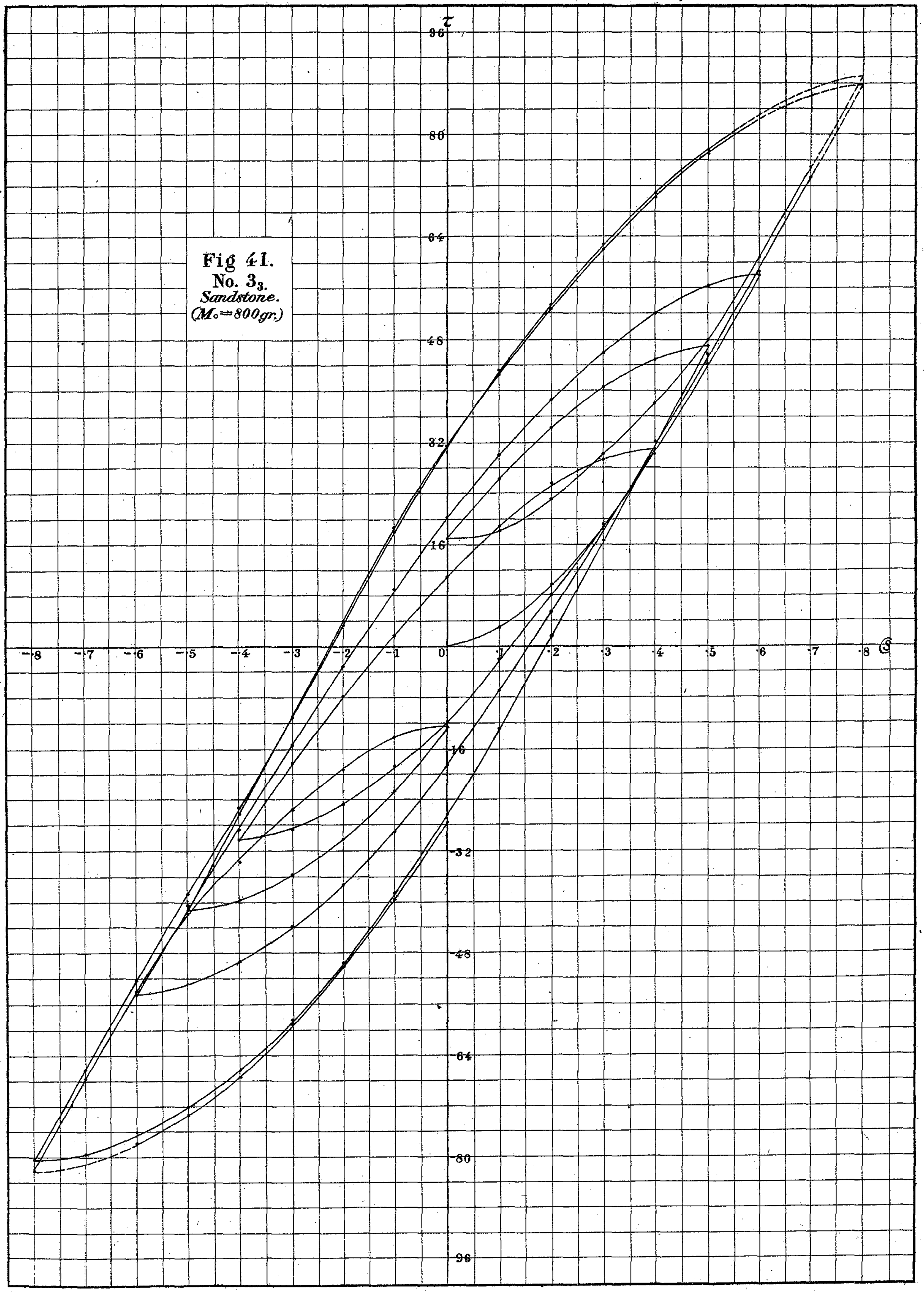
Fig 41.
No. 3₃.
Sandstone.
(M₀=800gr.)
τ
96
80
64
48
32
16
-16
-32
-48
-64
-80
-96
-·8
-·7
-·6
-·5
-·4
-·3
-·2
-·1
0
·1
·2
·3
·4
·5
·6
·7
·8
S

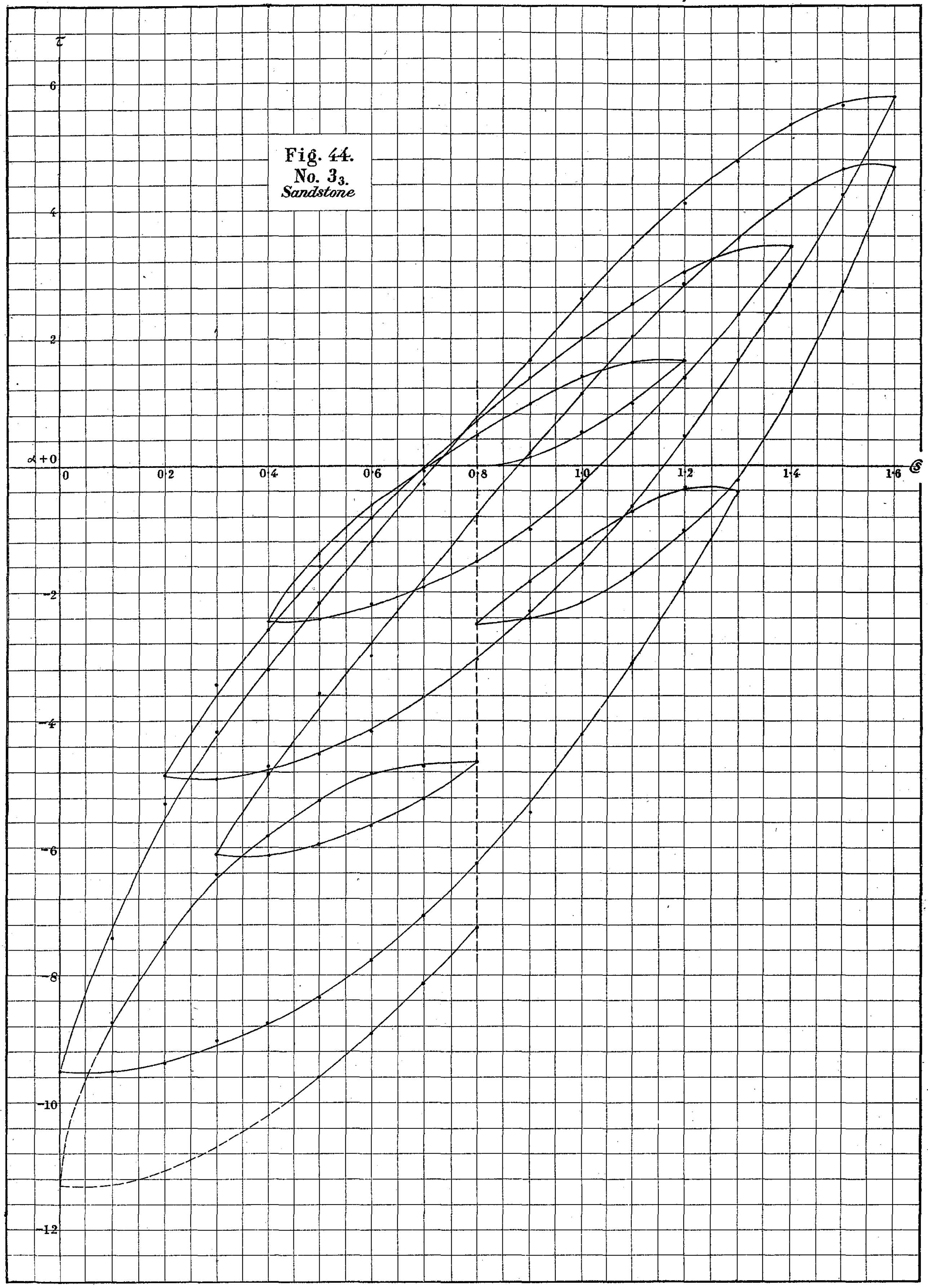
Fig. 44.
No. 3_3.
Sandstone
τ
6
4
2
α + 0
-2
-4
-6
-8
-10
-12
0
0·2
0·4
0·6
0·8
1·0
1·2
1·4
1·6
S

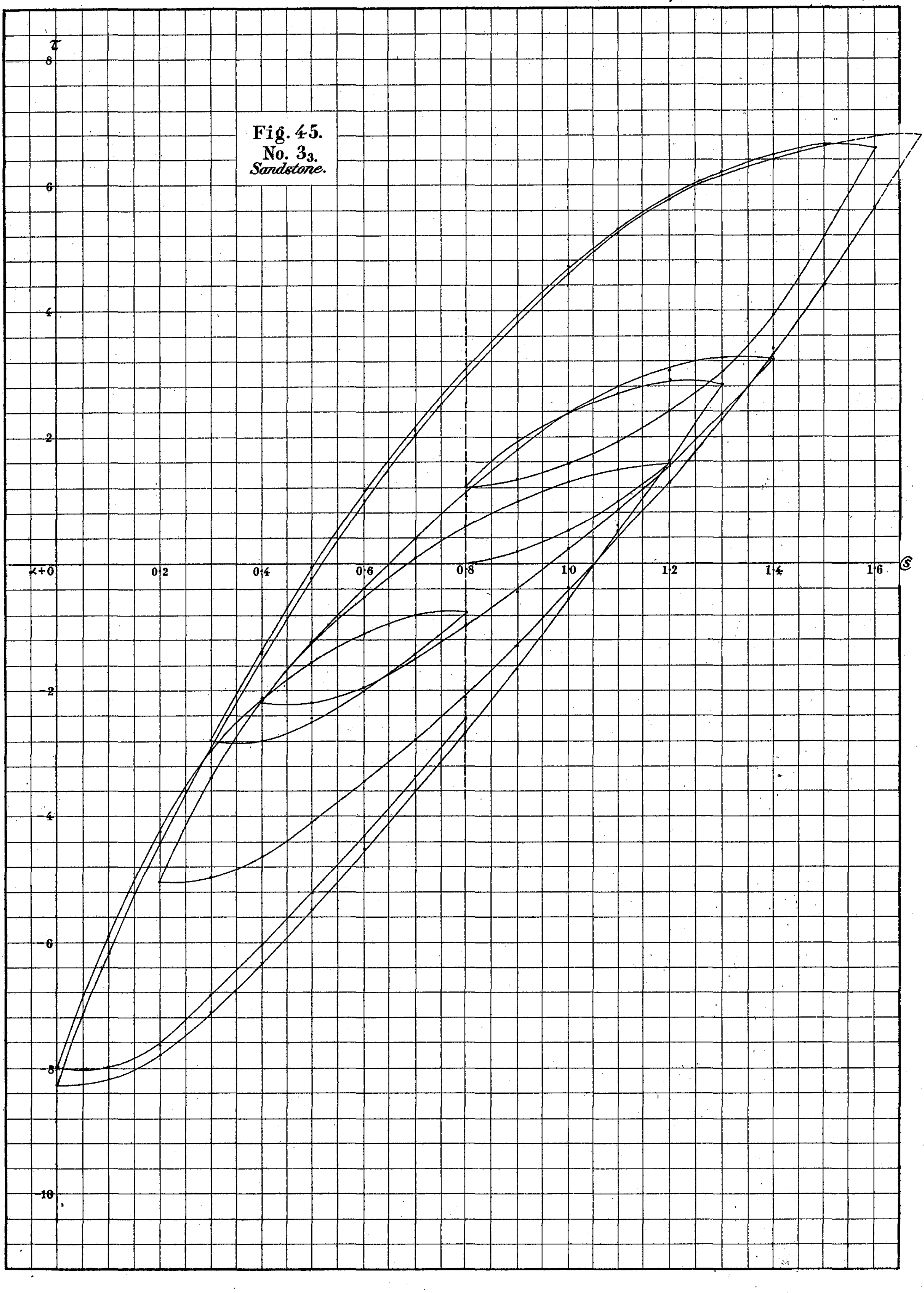
Fig. 45.
No. 3_3.
Sandstone.
τ
8
6
4
2
−2
−4
−6
−8
−10
+0
0·2
0·4
0·6
0·8
1·0
1·2
1·4
1·6
S

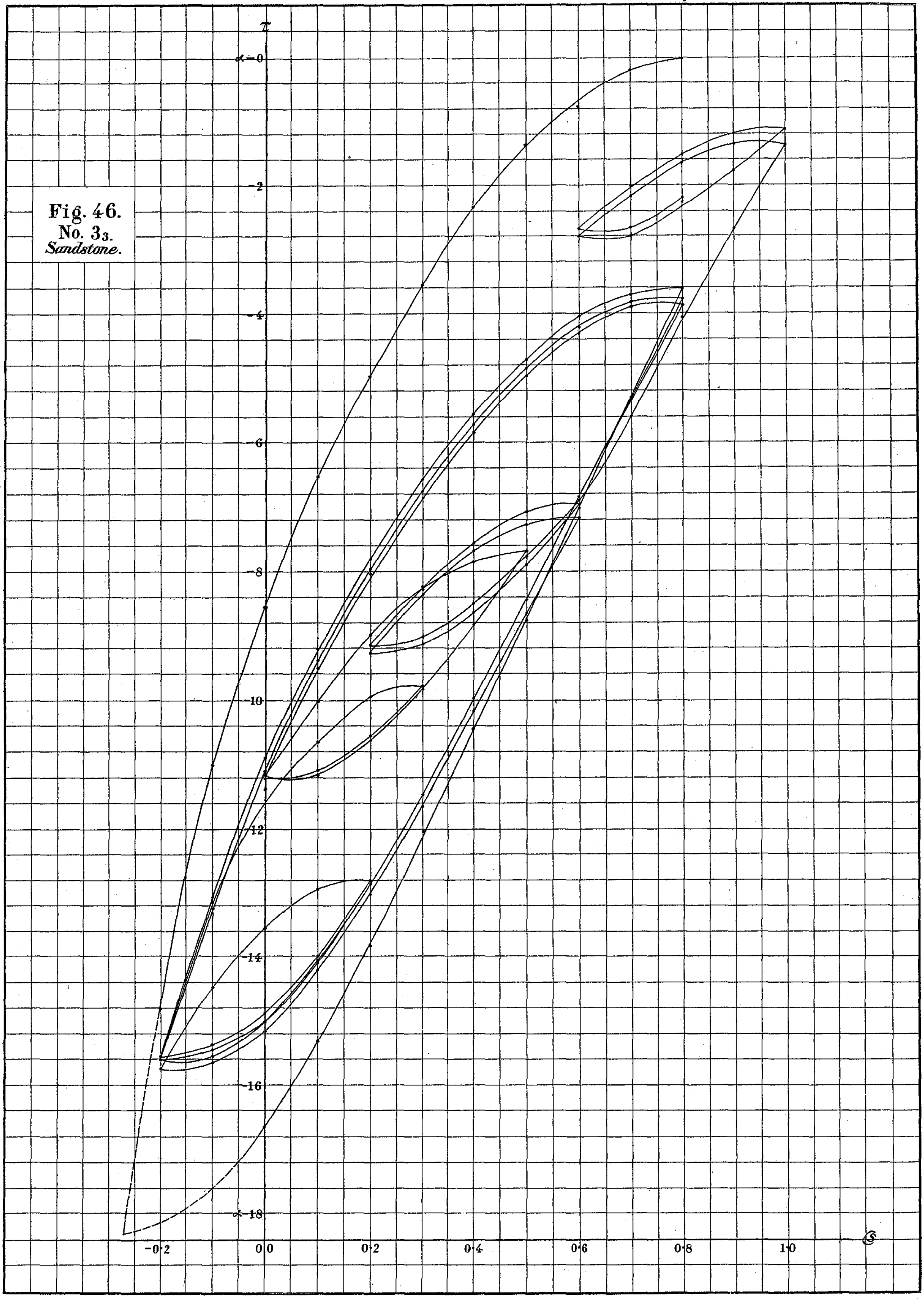
Fig. 46.
No. 3₃.
Sandstone.
π
-0
-2
-4
-6
-8
-10
-12
-14
-16
-18
-0·2
0·0
0·2
0·4
0·6
0·8
1·0
S

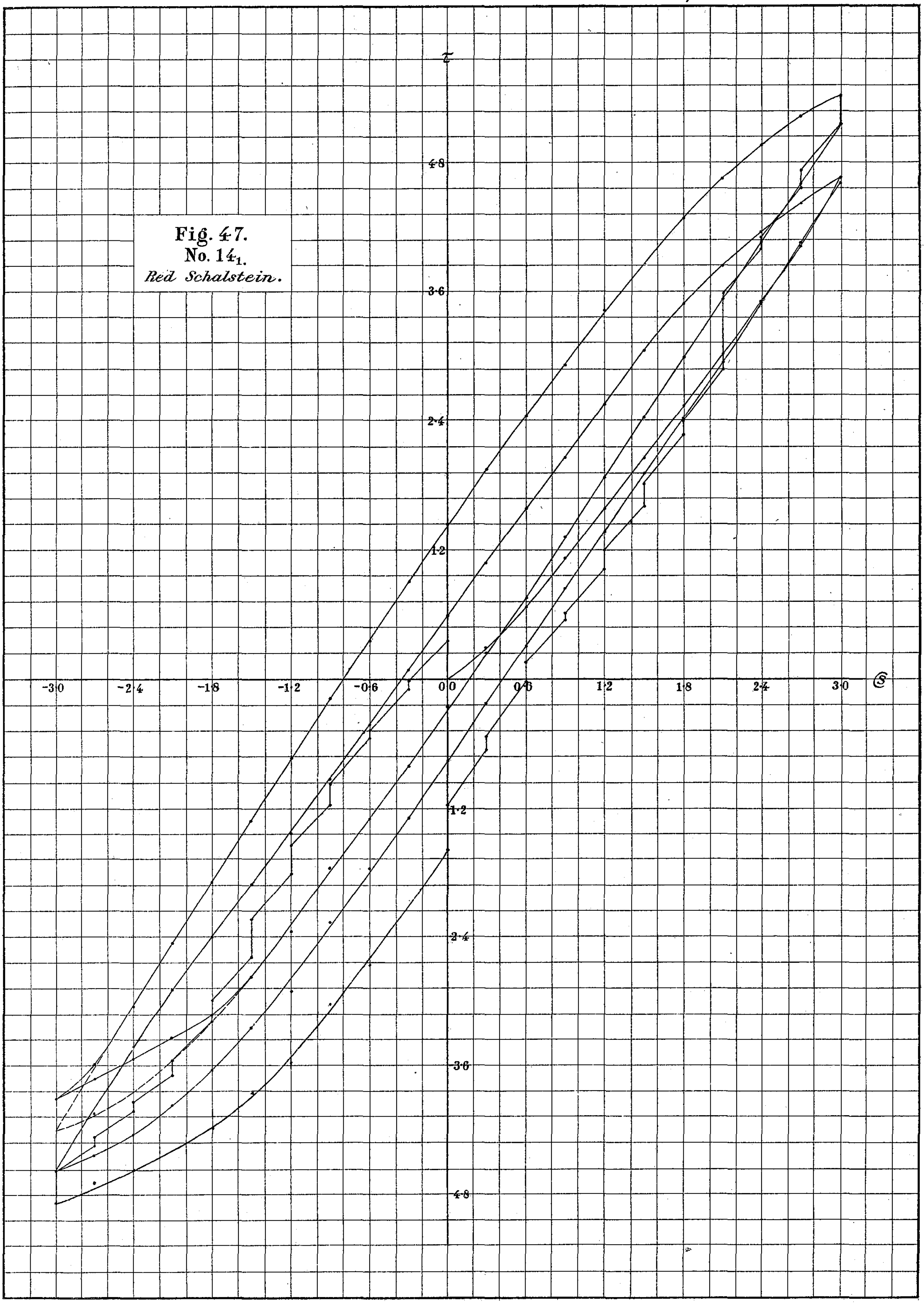
Fig. 47.
No. 14_1.
Red Schalstein.
τ
4·8
3·6
2·4
1·2
-3·0
-2·4
-1·8
-1·2
-0·6
0·0
0·6
1·2
1·8
2·4
3·0
𝔖
1·2
2·4
3·6
4·8

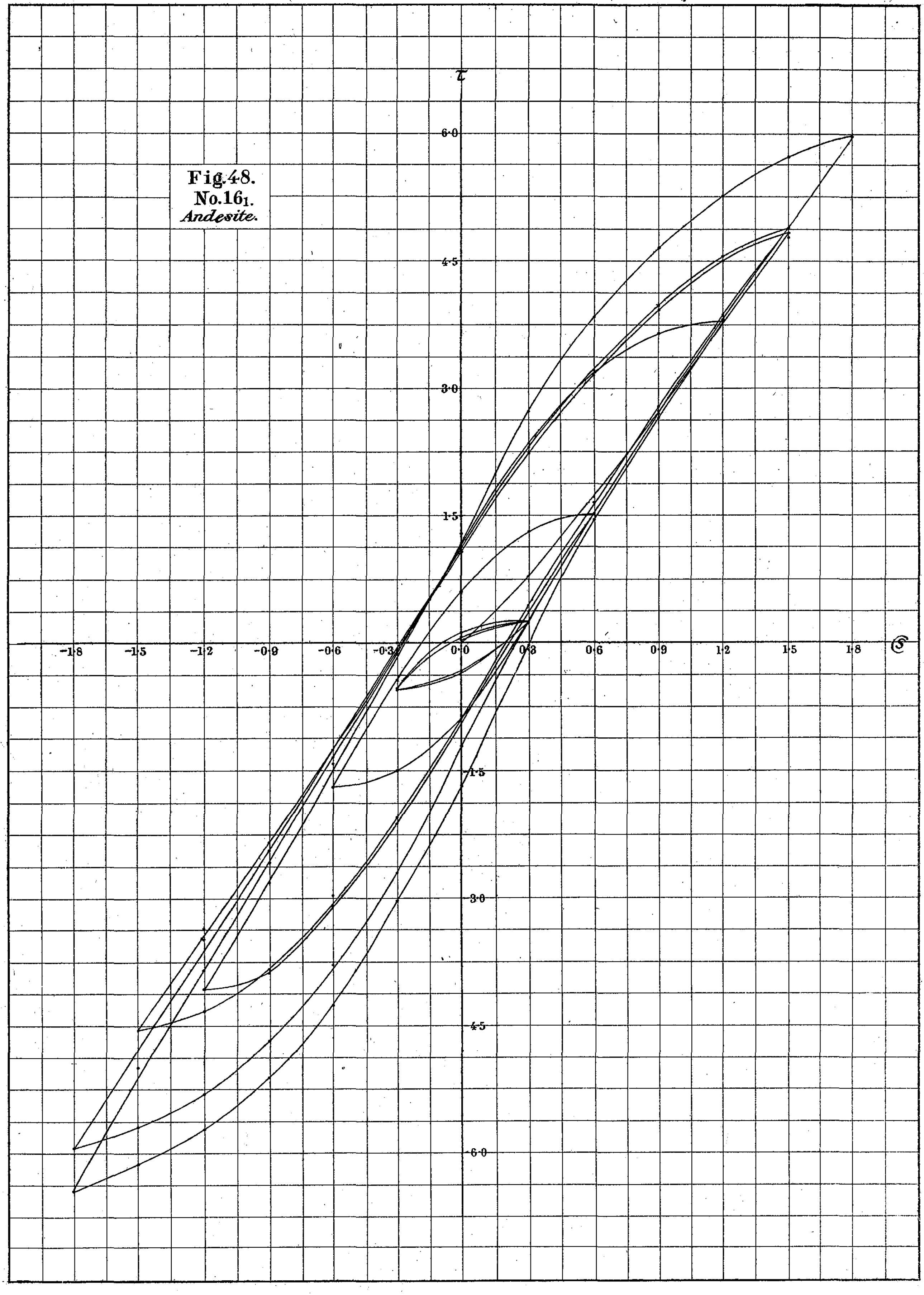
Fig. 48.
No. 16_1.
Andesite.
τ
6·0
4·5
3·0
1·5
−1·8
−1·5
−1·2
−0·9
−0·6
−0·3
0·0
0·3
0·6
0·9
1·2
1·5
1·8
S
1·5
3·0
4·5
6·0

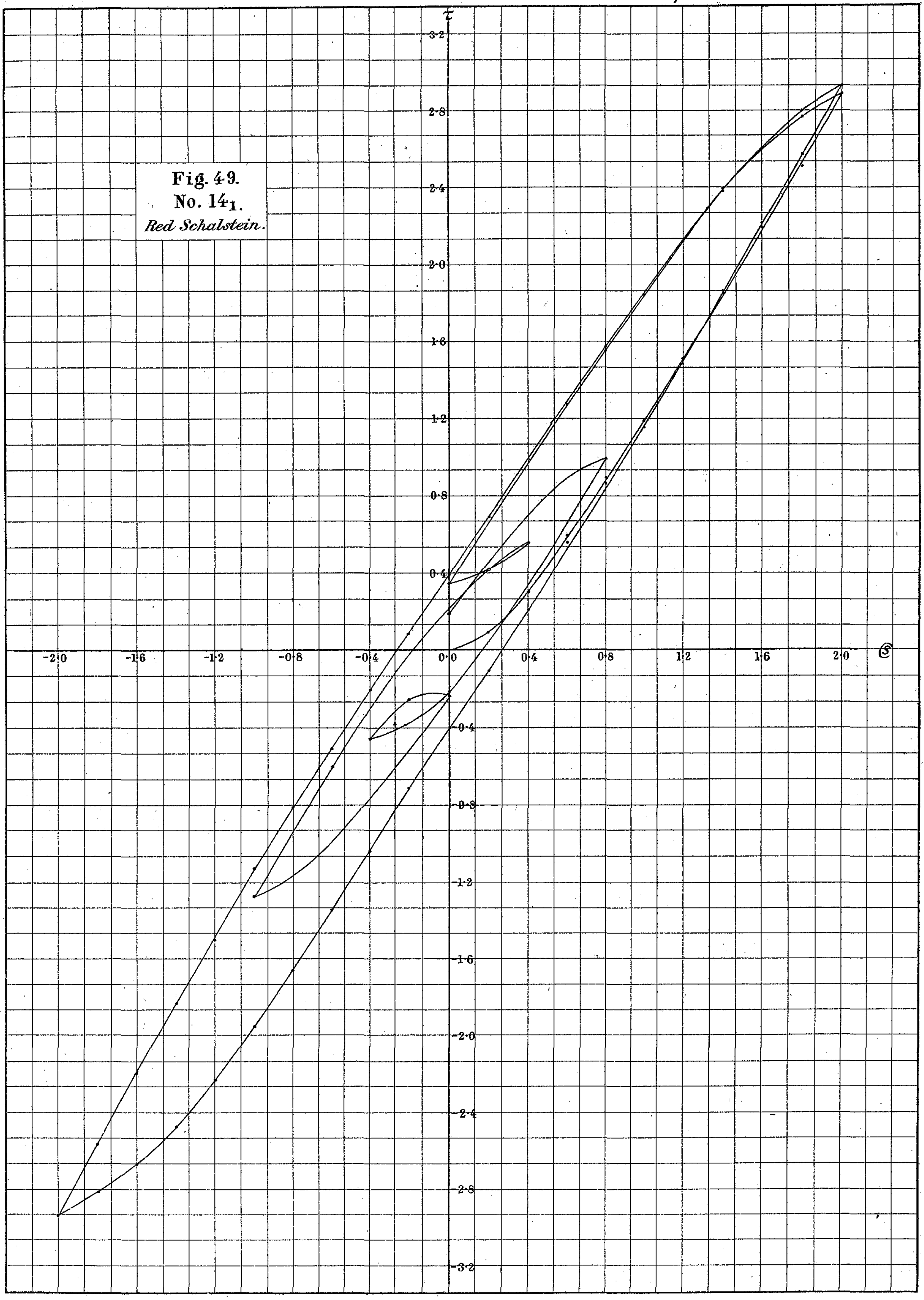
Fig. 49.
No. 14_1.
Red Schalstein.
τ
3·2
2·8
2·4
2·0
1·6
1·2
0·8
0·4
0·0
-0·4
-0·8
-1·2
-1·6
-2·0
-2·4
-2·8
-3·2
-2·0
-1·6
-1·2
-0·8
-0·4
0·4
0·8
1·2
1·6
2·0
𝔖

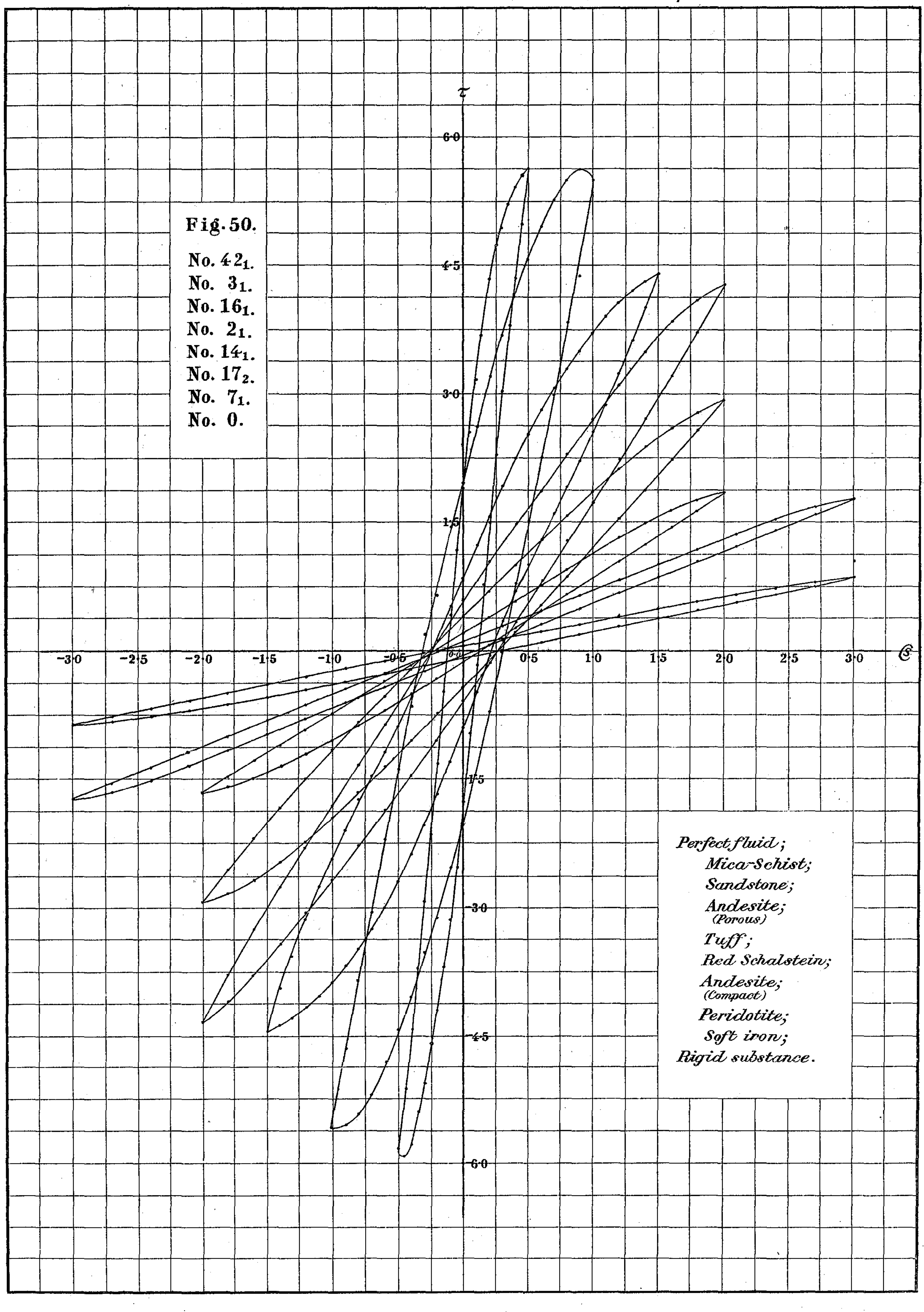
Fig. 50.
No. $4\,2_1$.
No. 3_1.
No. 16_1.
No. 2_1.
No. 14_1.
No. 17_2.
No. 7_1.
No. 0.
Perfect fluid;
Mica-Schist;
Sandstone;
Andesite; (Porous)
Tuff;
Red Schalstein;
Andesite; (Compact)
Peridotite;
Soft iron;
Rigid substance.
τ
6·0
4·5
3·0
1·5
-1·5
-3·0
-4·5
-6·0
-3·0
-2·5
-2·0
-1·5
-1·0
-0·5
0·0
0·5
1·0
1·5
2·0
2·5
3·0
S

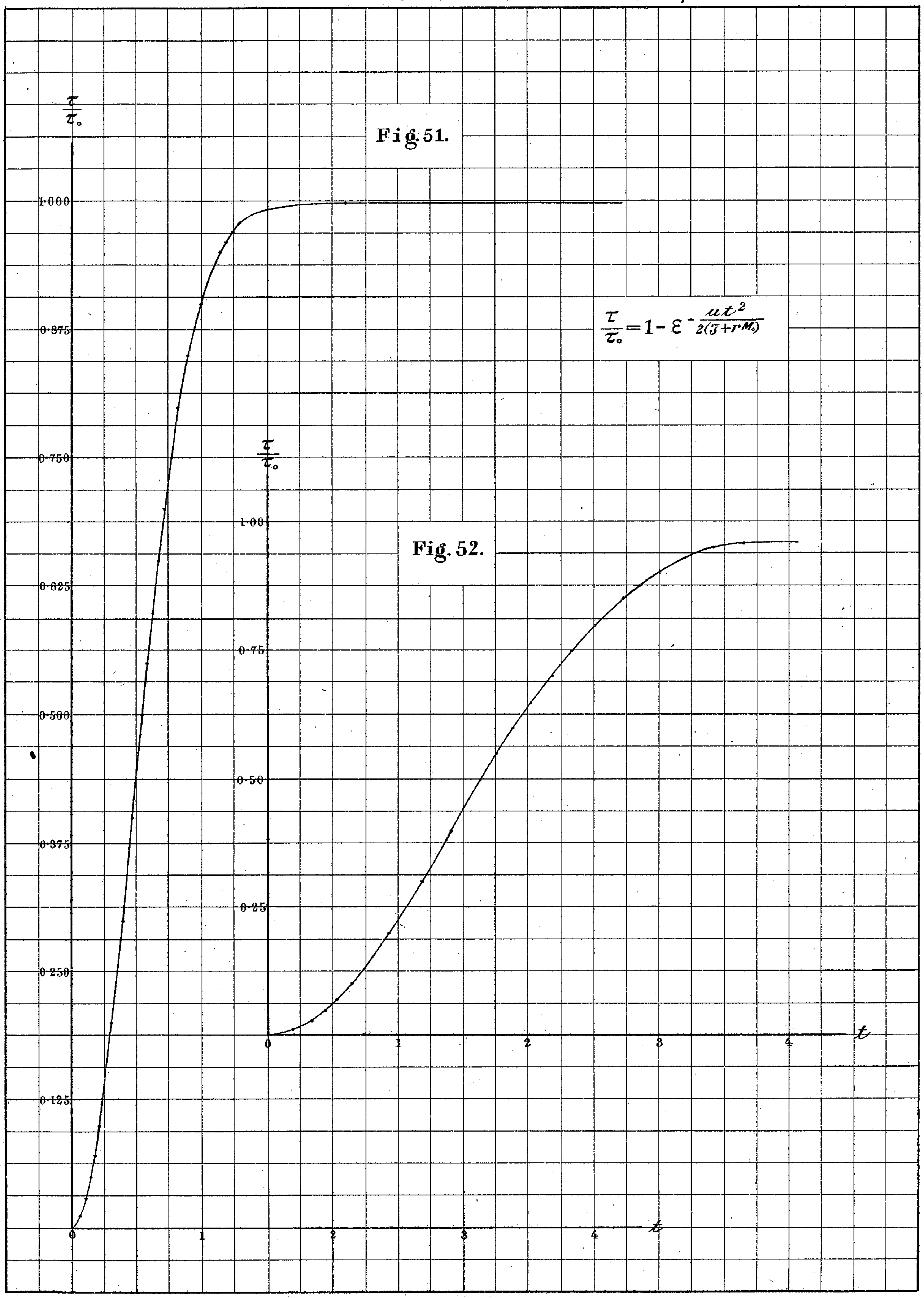
Fig. 51.
Fig. 52.
$\frac{\tau}{\tau_0} = 1 - \varepsilon^{-\frac{ut^2}{2(\mathfrak{J}+rM_0)}}$
$\frac{\tau}{\tau_0}$
1·000
0·875
0·750
0·625
0·500
0·375
0·250
0·125
1·00
0·75
0·50
0·25
0
1
2
3
4
t

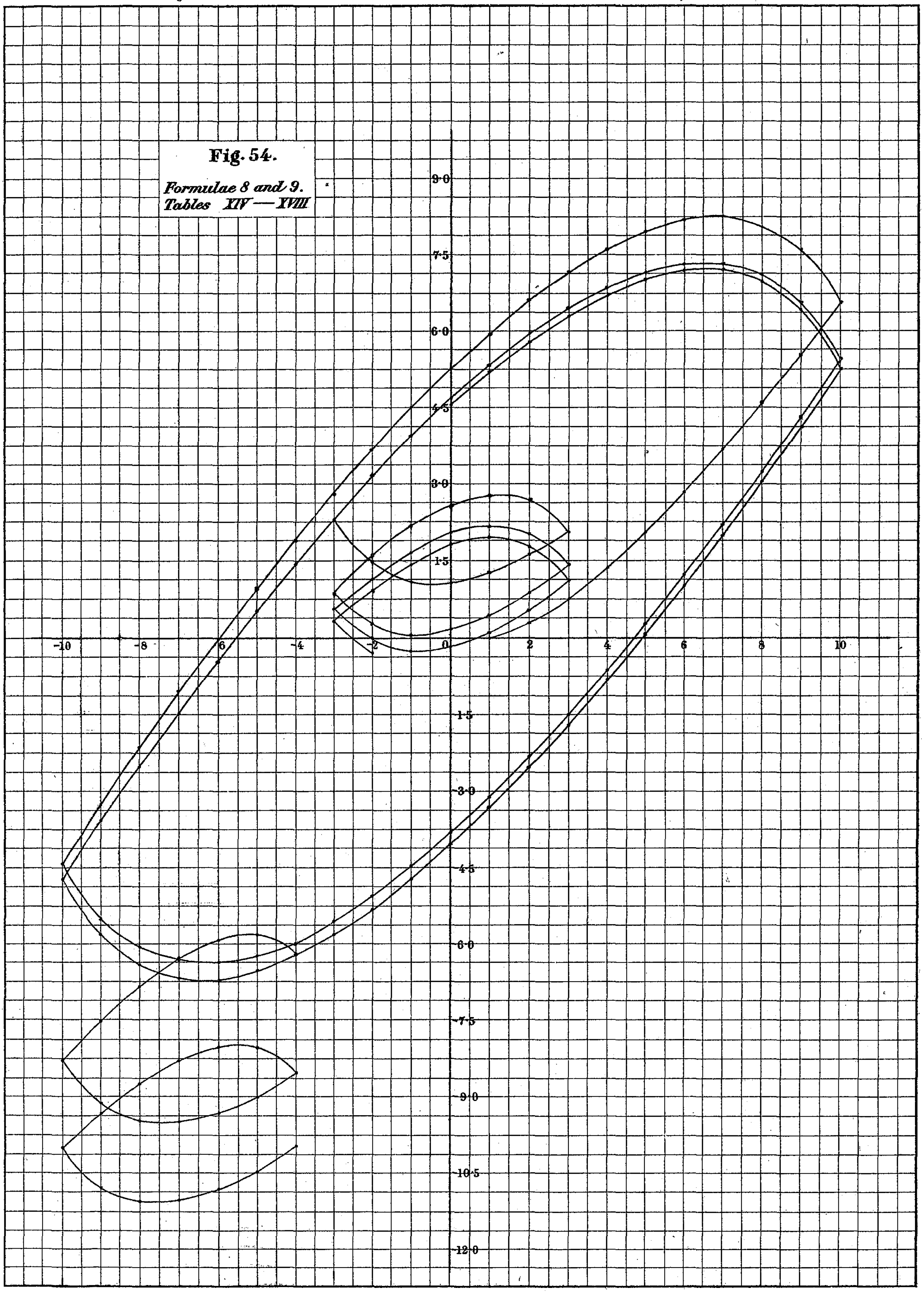
Fig. 54.
Formulae 8 and 9.
Tables XIV — XVIII
9·0
7·5
6·0
4·5
3·0
1·5
-10
-8
-6
-4
-2
0
2
4
6
8
10
-1·5
-3·0
-4·5
-6·0
-7·5
-9·0
-10·5
-12·0

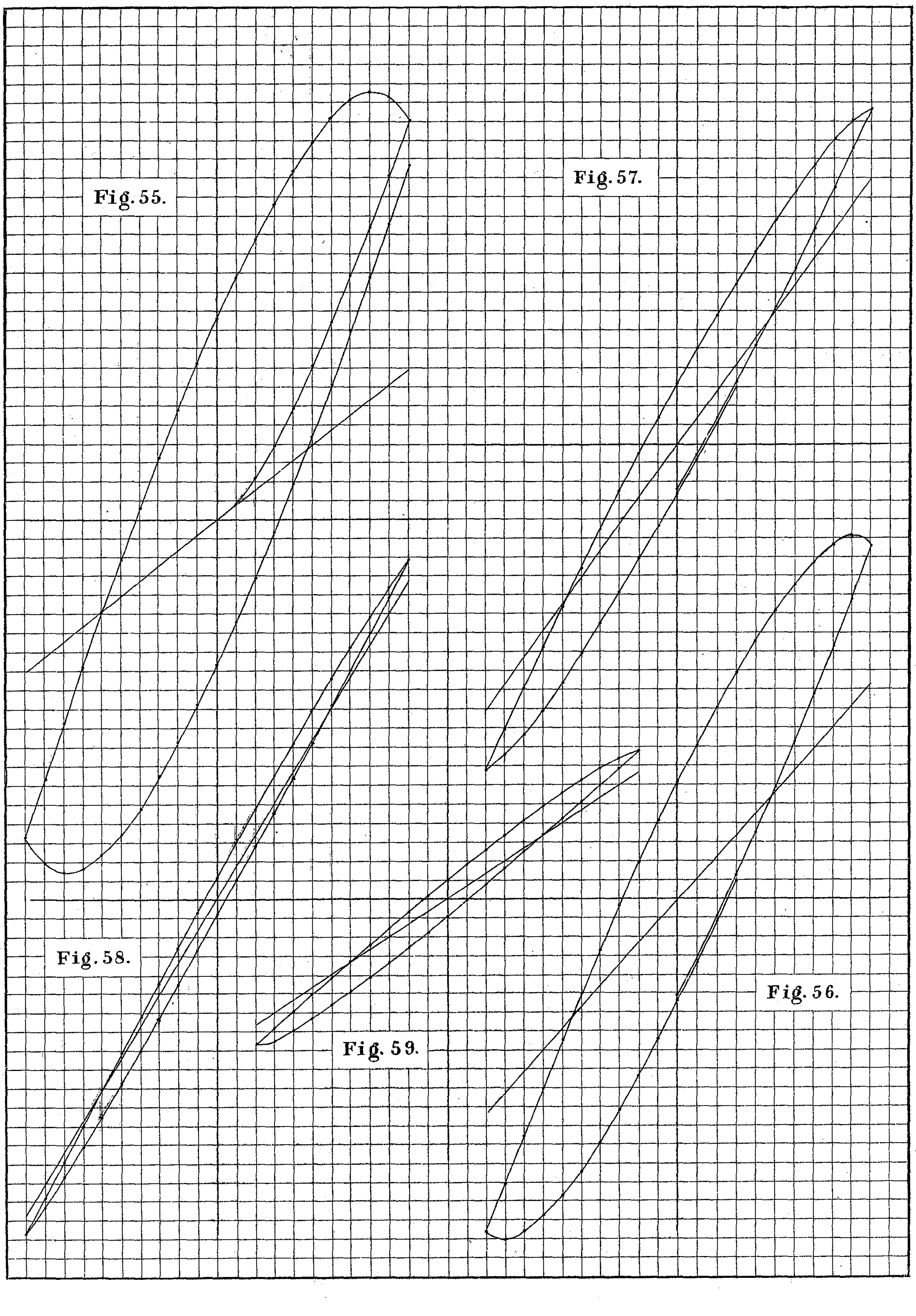
Fig. 55.
Fig. 57.
Fig. 58.
Fig. 59.
Fig. 56.